THE EFFECTS OF CHANGING THE COMPOSITION OF A MIXED MOBILE PHASE IN ELECTROCHEMICALLY MODULATED LIQUID CHROMATOGRAPHY

by

Jennifer Ann Williams

A thesis submitted to the faculty of
The University of Utah
in partial fulfillment of the requirements for the degree of

Master of Science

Department of Chemistry

The University of Utah

August 2011

The University of Utah Graduate School

STATEMENT OF THESIS APPROVAL

The thesis of **Jennifer Ann Williams**

has been approved by the following supervisory committee members:

Marc D. Porter	, Chair	**05/12/2011** Date Approved
Michael H. Bartl	, Member	**05/12/2011** Date Approved
Joel S. Miller	, Member	**05/12/2011** Date Approved

and by **Henry S. White** , Chair of the Department of **Chemistry**

and by Charles A. Wight, Dean of The Graduate School.

ABSTRACT

The research presented in this thesis investigates the effect of the organic modifier, acetonitrile (ACN), as an additive to an aqueous mobile phase on the electrosorption of aromatic sulfonates onto porous graphitic carbon (PGC), as probed by electrochemically modulated liquid chromatography (EMLC). EMLC is a technique that employs a conductive material such as PGC as both the stationary phase and the working electrode. This dual functionality enables the manipulation of chromatographic retention by changing the potential applied to the stationary phase. This change alters the electrosorption process at the solid-liquid interfaces. Previous works have investigated these changes by applying the Gibbs adsorption equation to determine the interfacial excess (Γ), surface tension ($d\gamma$), and surface charge (q^M). This thesis incorporates the Gibbs adsorption equation to evaluate the effect ACN has on the electrosorption of aromatic sulfonates. This study is then followed up by using attenuated total reflection FTIR spectroscopy (ATR-FTIRS) to study the interactions in the mobile phase of this system, which consisted of mixed water:acetonitrile solutions with benzene as the solute and lithium perchlorate ($LiClO_4$) as the supporting electrolyte.

TABLE OF CONTENTS

LIST OF FIGURES

Figure Page

ABBREVIATIONS

1,3-BDS.....disodium 1,3-benzenedisulfonate

1,5-NDS.....disodium 1,5-naphthalenedisulfonate

2,6-NDS.....disodium 2,6-napthalenedisulfonate

A.....surface area

ACN.....acetonitrile

Ag/AgCl/saturated NaCl.....silver/silver chloride/saturated sodium chloride

ATR.....attenuated total reflection

BDDP.....boron-doped diamond particles

BS.....sodium benzenesulfonate

$d\gamma$.....surface tension

E_{app}.....potential applied

EDL.....electrical double layer

EMLC.....electrochemical modulated liquid chromatography

FTIRS.....fourier transform infrared spectroscopy

G-C theory.....Gouy-Chapman theory

GC.....glassy carbon

HPLC.....high performance liquid chromatography

i.....ions

IHP.....inner Helmholtz plane

k'.....capacity factor

$LiClO_4$.....lithium perchlorate

n_s.....number of moles on the stationary phase

n_m.....number of moles in the mobile phase

n_{tot}.....total number of moles

$NaPF_6$.....sodium hexafluorophosphate

OHP.....outer Helmholtz plane

PGC.....porous graphitic carbon

PREG.....polar retention effect by graphite

PZC.....potential zero charge

q^M.....electrode charge

t_o.....unretained peak

t_r.....retention time

ZnSe.....zinc selenide

Γ.....interfacial excess

μ.....chemical potential

ACKNOWLEDGEMENTS

I would like to show my gratitude and extend my sincere appreciation to those who have made this thesis possible. First and foremost, I would like to thank my major advisor Marc Porter. Thank you for your guidance, patience, and advice. Also, to extend my appreciation to the research scientists Mike Granger, Jennifer Granger, and Lorraine Spierko for providing your expertise when it was needed. Another special thank you is to Bev Warner for your help with writing and with whatever else that was needed.

I am also grateful for the Porter research group members both past and present. In particular, I would like to thank Heeyeon (Hannah) Park Wampler for her support, guidance, friendship, and her unbelievable amount of patience. I am also grateful for the most supportive friendships that I know will last a lifetime: Brian Ehlert, Lexi Crawford, and Nikka Bradley. Another thank you is to Ron Wampler, for always willing to answer my never-ending questions along with the never-ending proofreading.

To the people who have supported me all this way and will continue to do so throughout my life are of course my parents and siblings. To my mother and father whom have taught me to work hard and to never give up. Who showed me to be tough, persistent, and diligent. For always allowing me to put education first and foremost. To my biggest inspiration, my sister who has and continues to show me to let yourself be "blown in the wind." To my brother, who has taught me to work hard, but to enjoy the simple things in life. Lastly, to my best friend, thank you for your patience and support.

CHAPTER 1

GENERAL INTRODUCTION

1.1 Thesis Overview and Organization

This thesis examines the effect an organic modifier has on the current mechanistic understanding of electrosorption on porous graphitic carbon (PGC) as examined by electrochemically modulated liquid chromatography. In this chapter, a review of EMLC, the PGC stationary phase, retention mechanisms, and the electrical double layer is presented.

Following this overview, the second chapter investigates aromatic sulfonates as test solutes with respect to changes in retention with changes in acetonitrile concentration. This chapter extends the understanding of this process by analyzing the potential zero charge (PZC), interfacial excess (Γ), and surface tension ($d\gamma$). The subsequent chapter provides details of interactions occurring within the mobile phase as examined by infrared spectroscopy in an internal reflectance mode. Specifically, benzene, a neutral aromatic, was studied in various ratios of a water:acetonitrile solution containing the supporting electrolyte, lithium perchlorate ($LiClO_4$), to understand the interactions occurring in bulk solution. These research chapters are followed by a summary and conclusions of the work presented herein.

1.2 Literature Review

1.2.1 EMLC Overview

Electrochemically modulated liquid chromatography (EMLC) is a unique combination of high performance liquid chromatography (HPLC) and electrochemistry.[1] To optimize a separation in HPLC, the stationary phase can be changed and/or the mobile phase composition can be altered depending on the sample. EMLC was developed to overcome these changes by configuring an HPLC column to act as a three-electrode electrochemical cell. An EMLC column consists of a conductive packing material (e.g., glassy carbon (GC), porous graphitic carbon (PGC), or boron-doped diamond particles (BDDP)) that functions both as the stationary phase and working electrode. Manipulation of a separation can therefore be achieved by altering the surface charge density of the conductive packing by altering the applied potential (E_{app}).

1.2.2 Stationary Phases

Carbon-based stationary phases have been widely used in liquid chromatography. In early studies, several carbonaceous stationary phases were developed for HPLC.[2,3] The first reported use of carbon as a stationary phase was by Kiselev and coworkers in which silica gel particles were coated with pyrolytic carbon.[4,5] At the same time, Guiochon and coworkers modified carbon black particles and found them to possess attractive properties for separations.[6-8] Since then, several efforts have been devoted to improving carbon-based HPLC stationary phases.[9-14] A majority of these carbons, however, were not suitable for HPLC because of weak mechanical strength, wide pore-size distrubtion, or a surface composed of other chemical species besides carbon.[14-17] Recently, Knox and

Gilbert introduced porous glassy carbon (PGC) laying the foundation for a much more efficient stationary phase[18,19] that was found to be applicable for a wide variety of separations based upon a retention mechanism distinct from conventional reversed phases.[20-22]

1.2.3 Porous Graphitic Carbon

PGC possesses very specific properties that are ideal for EMLC separations. PGC is mechanically strong and can withstand pressures up to 8000 psi. It is chemically inert and insensitive to aggressive mobile phases with extreme pH and other harsh properties. This packing also has a high surface area (~150 $m^2 g^{-1}$) and a high inherent electrical conductivity (≥100 S/cm).[1] This allows for both efficient chromatographic separations and operation as a working electrode. PGC is reproducibly prepared and commercially available as tightly disperse, miron-sized particles (e.g., Hypercarb®). The porosity of PGC is 80%, with an average pore diameter of 250 Å. [1,21-25]

PGC is made up of intertwined graphitic ribbons with each ribbon consisting of ~30 sheets. These sheets are of hexagonal arrangement with sp^2-hybridized carbon atoms. The carbon atoms are roughly 1.40 Å apart and held together through covalent bonds. The sheets are separated by about 3.4 Å with van der Waals interactions keeping the sheets intact.[10,11,26] It is this unique structure that accounts for the mechanical strength of PGC. Its efficient use in chromatographic separations is due to its almost homogeneous surface. Through X-ray photoelectron spectroscopy (XPS), the PGC surface is determined to be roughly composed 0.14 atomic percent oxygen, largely of phenol, carbonyl, carboxylic acid, lactone, and quinone groups. As might be expected, changes in surface oxygen groups have been shown to alter retention.[22,27-29]

Blaedel and Strohl were the first to apply a potential to carbonaceous packings.[30] Selectivity was shown to be somewhat affected by E_{app}. Since then, EMLC, a new form of HPLC has come into use.[1] These later works, through a new column design, showed that retention is dependent upon E_{app} and that a column can be built to function with separation efficiency comparable in HPLC.[30-37] Indeed, our group performed several studies on modification of the column to achieve efficient separations for a wide variety of solutes such as aromatic sulfonates,[38,39] monosubstituted benzenes,[40] corticosteroids,[41] benzodiazepines,[42] and amino acids.[43]

1.2.4 EMLC Columns

A schematic of an EMLC column is shown in Figure 1-1.[44] The design of the column consists of a porous stainless steel cylinder lined with a tubular Nafion® cation-exchange membrane. The stainless steel functions as a high surface area auxiliary electrode to carry the current from the high surface area working electrode and as a rigid support for the Nafion tubing to withstand the high pressures applied during packing and chromatographic flow. The cation-exchange membrane functions as: (1) a salt bridge for ion transport between the stationary phase and the other electrodes; (2) a container for the stationary phase to prevent loss of analyte through the porous stainless steel cylinder and to prevent possible contamination of the stationary phase from any electrolysis products that may form at the auxiliary electrode; and (3) an electronic insulator between the working and auxiliary electrode. The stationary phase is slurry-packed into the column.

The working electrode is electrically connected via a stainless steel frit at the bottom of the column. An electrolyte-filled reservoir is fitted around the column, more specifically the porous stainless steel, to house a reference electrode (e.g.,

Ag/AgCl/saturated NaCl). The poly(ether ether ketone) (PEEK) union connects the top and bottom of the column and the Kel-F ring electrically isolates the bottom of the column (working electrode) from the top of the column (auxiliary electrode). To complete the column, standard HPLC endfittings are applied to provide an electrical connection to a high-power potentiostat which controls E_{app}.

1.2.5 Retention/Electrosorption Mechanism

Chromatographic retention is defined as the partitioning of solutes between a mobile and stationary phase. Several models have been developed to describe chromatographic retention through interactions between: (a) the solute and stationary phase, (b) solute and mobile phase, and (c) mobile and stationary phases.[13,21,45-50] In contrast to conventional reversed phase materials, graphite exhibits stereochemical selectivity[51] and a stronger retention for polar solutes. The latter is termed the polar retention effect by graphite (PREG).[21,52-54] The strength of solute and stationary phase interactions is dependent not only on geometric factors but also on the polarizability of the PGC.[55,56] More to the point, retention at PGC arises from a combination of electrostatic and nonelectrostatic interactions. These interactions represent a complex mixing of dispersion, solvophobic, and donor-acceptor interactions.[21,26]

Dispersion interactions are nonspecific interactions occurring between the solute and graphitic surface. With these interactions, an increase in retention is found when an alkyl chain substituent on benzene or other aromatic moiety is elongated.[57] A linear behavior is observed for retention with these interactions, as described by equation 1-1:[46]

$$\log k' = \log k'_0 + \alpha n \qquad (1\text{-}1)$$

where *k'* is the retention factor, α is the measure of change in retention as the alkyl chain length increases, *n* is the number of carbons in the chain, and k'_0 is the theoretical retention factor for benzene. These studies found PGC to be more sensitive to aromatics with long carbon chain functional then reversed phase packings.[46]

The composition of the mobile phase has been shown to affect retention through solute-solvent dispersive interactions, otherwise known as solvophobic interactions. The eluotropic strength of a single organic component mobile phase solvent has been studied with no observable change in retention;[7,10,13,17,25,58,59] however, when mixed in aqueous-organic solvent, the retention of small aromatic molecules will decrease with an increase in the concentration of the organic modifier. This relationship is described in equation 1-2:

$$\log k' = \log k_W - S\phi \qquad (1\text{-}2)$$

where *k'* is the capacity factor, k_W is the capacity factor when water is the mobile phase composition includes water, ϕ is the concentration of organic modifier, and *S* is the sensitivity of solute retention in response to the organic modifier concentration. These studies have shown the molecular polarity of the solutes does indeed affect retention.[54,57,60-65]

Donor-acceptor interactions occur between the n- and/or π-electrons of an analyte and the delocalized π-system at the carbon surface. The graphite surface can act as either a proton donor or electron acceptor, because of its high polarizablity. Donor-acceptor interactions consist of five components: the electrostatic interaction, the polarization

interaction, the exchange repulsion, the charge-transfer interaction, and a coupling term.[39] The electrostatic interaction includes interactions between permanent charges and dipoles. The polarization interaction consists of attractive interactions between permanent and induced dipoles. The exchange repulsion is defined as a short-range repulsive term in response to an interaction occurring between electron clouds of a donor and an acceptor. The charge-transfer interaction is an attractive interaction involving charge transfer from the highest occupied molecular orbital (HOMO) of a donor to the lowest unoccupied molecular orbital (LUMO) of an acceptor. The coupling term is predominantly a weak interaction occurring between a donor and an acceptor.[39]

EMLC uses E_{app} to alter the interfacial properties (e.g., surface charge, double layer structure, and oxidation state) of the stationary phase for manipulation of solute retention. Altering the polarity of a donor or acceptor involves changing the electrostatic interactions, as idealized in Figure 1-2.[38] This interaction is dependent upon E_{app} and the PZC. When E_{app} is positive of the PZC, the carbon stationary phase has a net positive surface excess charge causing retention for negatively-charged analytes to increase due to electrostatic interactions. A decrease in retention is observed when E_{app} is negative of the PZC, where the surface acquires a negative excess charge.[1,38-44,66-68]

The electrostatic interaction is revealed when k' for a solute is plotted as ln k' against E_{app}. When a linear dependence is observed, the retention can be explained simply by the Boltzmann distribution of ions.[1] When a nonlinear relationship is observed, other factors become important such as donor-acceptor and solvophobic interactions.[69] To further understand interactions at the surface, the electrified interface and electrosorption process were investigated by applying the Gibbs adsorption equation and

the Lippmann equation to determine interfacial excess (Γ), changes in surface tension ($d\gamma$), charge of the electrode (q^M), and the PZC.[70] These interfacial properties gave insight into the factors that control the strength of specific adsorption.

The retention mechanism is explained through two models: (1) partition[71] and (2) adsorption.[63] The partition model describes solute retention based on its distribution between the mobile phase and the solvent layer on the stationary phase. The adsorption model describes adsorption sites on the surface of the stationary phase in which a solute molecule will displace adsorbed solvent molecules. A combination of these models, applied on a case-by-case basis, provides a qualitative explanation for retention manipulated by EMLC.[72]

1.2.6 Electrical Double Layer

Solute retention in EMLC is further explained by the electrical double layer (EDL) theory. This theory explains how a solute orients itself on a charged surface through specific or nonspecific adsorption. The distribution of charge is simplified with the Gouy-Chapman (G-C) theory where the Helmholtz electrical double layers are defined, shown schematically in Figure 1-3.[73] The electrode-solution interface consists of the compact layer and the diffuse layer. The compact layer is described by the G-C theory, with the inner Helmholtz plane (IHP) composed of highly ordered solvent molecules and specifically adsorbed solutes; the outer Helmholtz plane (OHP) consists of solvated ions and solvent molecules. The diffuse layer is the layer between the OHP and the bulk solution where remaining charge is located to ensure electroneutrality of the interface. This theory can be used to understand the structure and distribution of charge at

the electrode-solution interface with the charges being either the solute or electrolyte molecules.[74,75]

Our laboratory has recently begun investigating the possibility of competition for adsorption sites between the solute and components of the mobile phase. The surface interactions and effects of the organic modifier are investigated in Chapter 2 and a direct analysis of the mobile phase is described in Chapter 3.

1.3 References

1. Harnisch, J. A.; Porter, M. D. *Analyst* **2001**, *126*, 1841-1849.

2. Tiselius, A. *Adv. Colloid Sci.* **1941**, *1*, 81-98.

3. Tiselius, A. *Adv. Protein Chem.* **1947**, *3*, 67-93.

4. Bebris, N. K.; Kiselev, A. V.; Nikitin, Y. S.; Frolov, I. I.; Tarasova, L. V.; Yashin, Y. I. *Chromatographia* **1978**, *11*, 206-211.

5. Bebris, N. K.; Vorobieva, R. G.; Kiselev, A. V.; Nikitin, Y. S.; Tarasova, L. V.; Frolov, I. I.; Yashin, Y. I. *J. Chromatogr.* **1976**, *117*, 257-268.

6. Colin, H.; Eon, C.; Guiochon, G. *J. Chromatogr.* **1976**, *122*, 223-242.

7. Colin, H.; Eon, C.; Guiochon, G. *J. Chromatogr.* **1976**, *119*, 41-54.

8. Colin, H.; Guiochon, G. *J. Chromatogr.* **1976**, *126*, 43-62.

9. Jackson, P. T.; Carr, P. W. *ChemTech* **1998**, *28*, 29-37.

10. Knox, J. H.; Kaur, B. *High Performance Liquid Chromatography Chemical Analysis*; Brown, P. R., Ed.; John Wiley & Sons, 1989; Vol. 98.

11. Knox, J. H.; Ross, P. *Advances in Chromatography*; Brown, P. R., Grushka, E., Eds.; Marcel Dekker Inc: New York, 1997; Vol. 37.

12. Knox, J. H.; Unger, K. K.; Mueller, H. *J. Liq. Chrom.* **1983**, *6*, 1-36.

13. Leboda, R.; Lodyga, A.; Charmas, B. *Mater. Chem. Phys.* **1998**, *55*, 1-29.

14. Liang, C.; Dai, S.; Guiochon, G. *Anal. Chem.* **2003**, *75*, 4904-4912.

15. Ciccioli, P.; Tappa, R.; Corcia, A. D.; Liberti, A. *J. Chromatogr.* **1981**, *206*, 35-42.

16. Plzak, Z.; Dousek, F. P.; Jansta, J. *J. Chromatogr.* **1978**, *147*, 137-142.

17. Unger, K. K.; Roumeliotis, P.; Mueller, H.; Goetz, H. *J. Chromatogr.* **1980**, *202*, 3-14.

18. Knox, J. H.; Gilbert, M. T. US Patent 4263268, 1979.

19. Gilbert, M. T.; Knox, J. H.; Kaur, B. *Chromatographia* **1982**, *16*, 138-146.

20. Bassler, B. J.; Hartwick, R. A. *J. Chromatogr. Sci.* **1989**, *27*, 162-165.

21. Ross, P. *LC GC North America* **2000**, *18*, 14.

22. West, C.; Elfakir, C.; Lafosse, M. *J. Chromatogr. A* **2010**, *1217*, 3201-3216.

23. Knox, J. H. *Chromatographia* **1996**, *42*, 83-88.

24. Unger, K. K. *Anal. Chem.* **1983**, *55*, 361-375.

25. Kaur, B. *LC GC Int.* **1990**, *8*, 472-477.

26. Knox, J. H.; Kaur, B.; Millward, G. R. *J. Chromatogr.* **1986**, *352*, 3-25.

27. McDermott, M. T.; McCreery, R. L. *Langmuir* **1994**, *10*, 4307-4314.

28. Ray, K. I.; McCreery, R. L. *Anal. Chem.* **1997**, *69*, 4680-4687.

29. Xu, J.; Chen, Q.; Swain, G. M. *Anal. Chem.* **1998**, *70*, 3146-3154.

30. Blaedel, W. J.; Strohl, J. H. *Anal. Chem.* **1964**, *36*.

31. Antrim, R. F.; Scherrer, R. A.; Yacynych, A. M. *Anal. Chim. Acta* **1984**, *164*, 283-286.

32. Ge, H.; Wallace, G. G. *Anal. Chem.* **1989**, *61*, 2391-2394.

33. Ghatak-Roy, A. R.; Martin, C. R. *Anal. Chem.* **1986**, *58*, 1574-1575.

34. Lam, P.; Elliker, P. R.; Wnek, G. E.; Przybycien, T. M. *J. Chromatogr. A* **1995**, *707*, 29-33.

35. Nagaoka, T.; Fujimoto, M.; Nakao, H.; Kakuno, K.; Yano, J.; Ogura, K. *J. Electroanal. Chem.* **1994**, *364*, 179-188.

36. Roe, D. K. *Anal. Chem.* **1964**, *36*, 2371-2372.

37. Suzuki, T.; Noble, R. D.; Koval, C. A. *Inorg. Chem.* **1997**, *36*, 136-140.

38. Deinhammer, R. S.; Ting, E.-Y.; Porter, M. D. *J. Electroanal. Chem.* **1993**, *362*, 295-299.

39. Deinhammer, R. S.; Ting, E.-Y.; Porter, M. D. *Anal. Chem.* **1995**, *67*, 237-246.

40. Ting, E.-Y.; Porter, M. D. *J. Electroanal. Chem.* **1998**, *443*, 180-185.

41. Ting, E.-Y.; Porter, M. D. *Anal. Chem.* **1997**, *69*, 675-678.

42. Ting, E.-Y.; Porter, M. D. *J. Chromatogr. A* **1998**, *793*, 204-208.

43. Deinhammer, R. S.; Porter, M. D.; Shimazu, K. *J. Electroanal. Chem.* **1995**, *387*, 35-46.

44. Ting, E.-Y.; Porter, M. D. *Anal. Chem.* **1998**, *70*, 94-99.

45. Hanai, T. *J. Chromatogr. A* **2003**, *989*, 183-196.

46. Kriz, J.; Adamcova, E.; Knox, J. H.; Hora, J. *J. Chromatogr. A* **1994**, *663*, 151-161.

47. Lepont, C.; Gunatillaka, A. D.; Poole, C. F. *Analyst* **2001**, *126*, 1318-1325.

48. Melander, W. R.; Horvath, C. *Chromatographia* **1984**, *18*, 353-361.

49. Vailaya, A.; Horvath, C. *J. Chromatogr. A* **1998**, *829*, 1-27.

50. Wang, A.; Tan, L. C.; Carr, P. W. *J. Chromatogr. A* **1999**, *848*, 21-37.

51. Burg, P.; Abraham, M. H.; Cagniant, D. *Carbon* **2003**, *41*, 867-879.

52. Bassler, B. J.; Kaliszan, R.; Hartwick, R. A. *J. Chromatogr.* **1989**, *461*, 139-147.

53. Kaliszan, R.; Osmialowski, K.; Bassler, B. J.; Hartwick, R. A. *J. Chromatogr.* **1990**, *499*, 333-344.

54. Hennion, M. C.; Coquart, V. *J. Chromatogr.* **1993**, *642*, 211-224.

55. Mockel, H. J.; Braedikow, A.; Melzer, H.; Aced, G. *J. Liq. Chromatogr.* **1991**, *14*, 2477-2498.

56. Tanaka, N.; Kimata, K.; Hosoya, K.; Miyanishi, H.; Araki, T. *J. Chromatogr. A* **1993**, *656*, 265-287.

57. Forgacs, E. *J. Chromatogr. A* **2002**, *975*, 229-243.

58. Colin, H.; Guiochon, G.; Jandera, P. *Chromatographia* **1982**, *15*, 133-139.

59. Eon, C. *Anal. Chem.* **1975**, *47*, 1871-1873.

60. Forgacs, E.; Cserhati, T. *Chromatographia* **1992**, *33*, 356-360.

61. Forgacs, E.; Cserhati, T.; Bordas, B. *Chromatographia* **1993**, *36*, 19-26.

62. Kaliszan, R. *Chem. Rev.* **2007**, *107*, 3212-3246.

63. Snyder, L. R. *Principles of Adsorption Chromatography*; Marcel Dekker Inc.: New York, 1968.

64. Coquart, V.; Hennion, M. C. *J. Chromatogr.* **1992**, *600*, 195-201.

65. Forgacs, E.; Cserhati, T. *J. Pharm. Biomed. Anal.* **1992**, *10*, 861-865.

66. Deng, H.; Van Berkel, G. J.; Takano, H.; Gazda, D.; Porter, M. D.; *Anal. Chem.* **2000**, *72*, 2641-2647.

67. Ho, M.; Wang, S.; Porter, M. D. *Anal. Chem.* **1998**, *70*, 4314-4319.

68. Wang, S.; Porter, M. D. *J. Chromatogr. A* **1998**, *828*, 157-166.

69. Pimienta, G. F. M.; Porter, M. D. *in preparation*.

70. Keller, D. W.; Porter, M. D. *Anal. Chem.* **2005**, *77*, 7399-7407.

71. Marin, A. J. P.; Synge, R. L. M. *Biochem. J* **1941**, *35*, 1358-1368.

72. Jaroniec, M. *J. Chromatogr. A* **1993**, *656*, 37-50.

73. Keller, D. W.; Ponton, L. M.; Porter, M. D. *J. Chromatogr. A* **2005**, *1089*, 72-81.

74. Bard, A. J.; Faulkner, L. R. *Electrochemical Methods: Fundamentals and Applications*; John Wiley & Sons, Inc.: New York, 2001.

75. Schmickler, W. *Chem. Rev*. **1996**, *96*, 3177-3200.

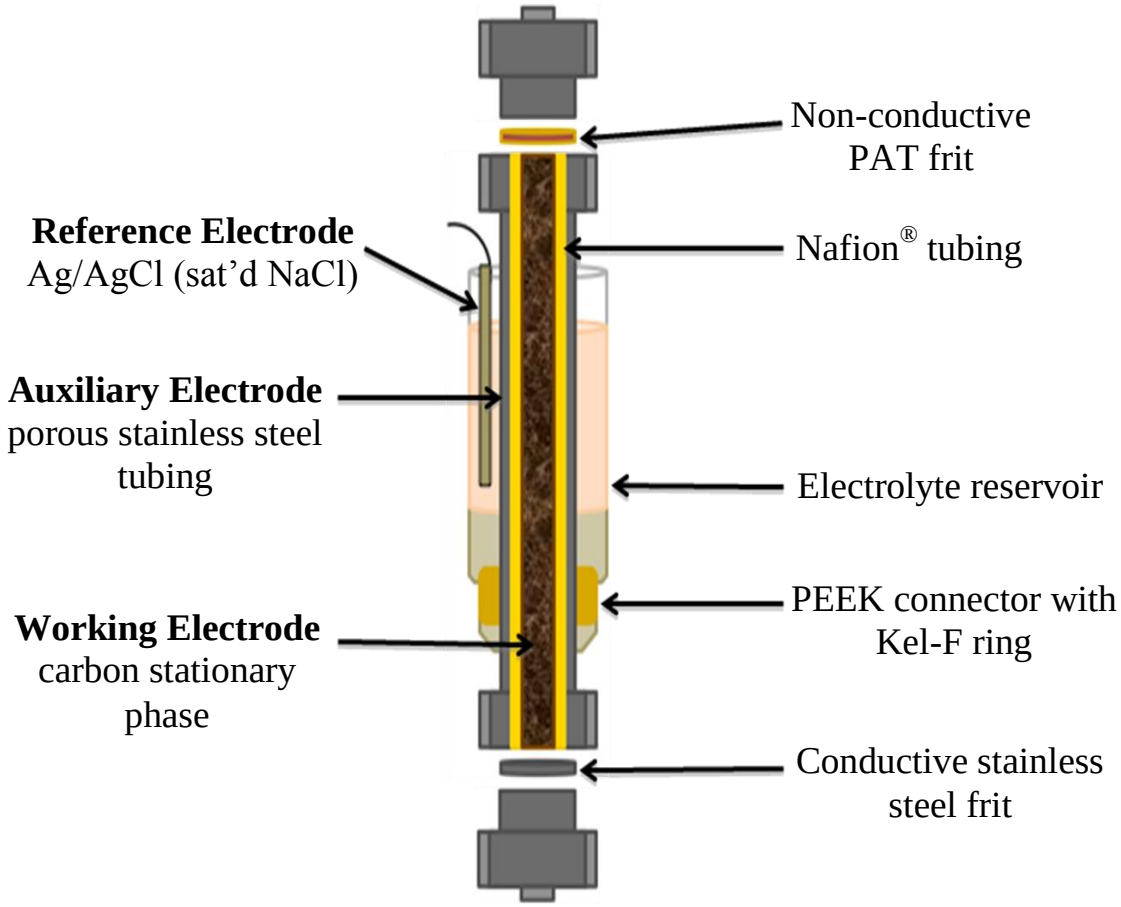

Figure 1-1. Schematic representation of the column for electrochemically modulated liquid chromatography.

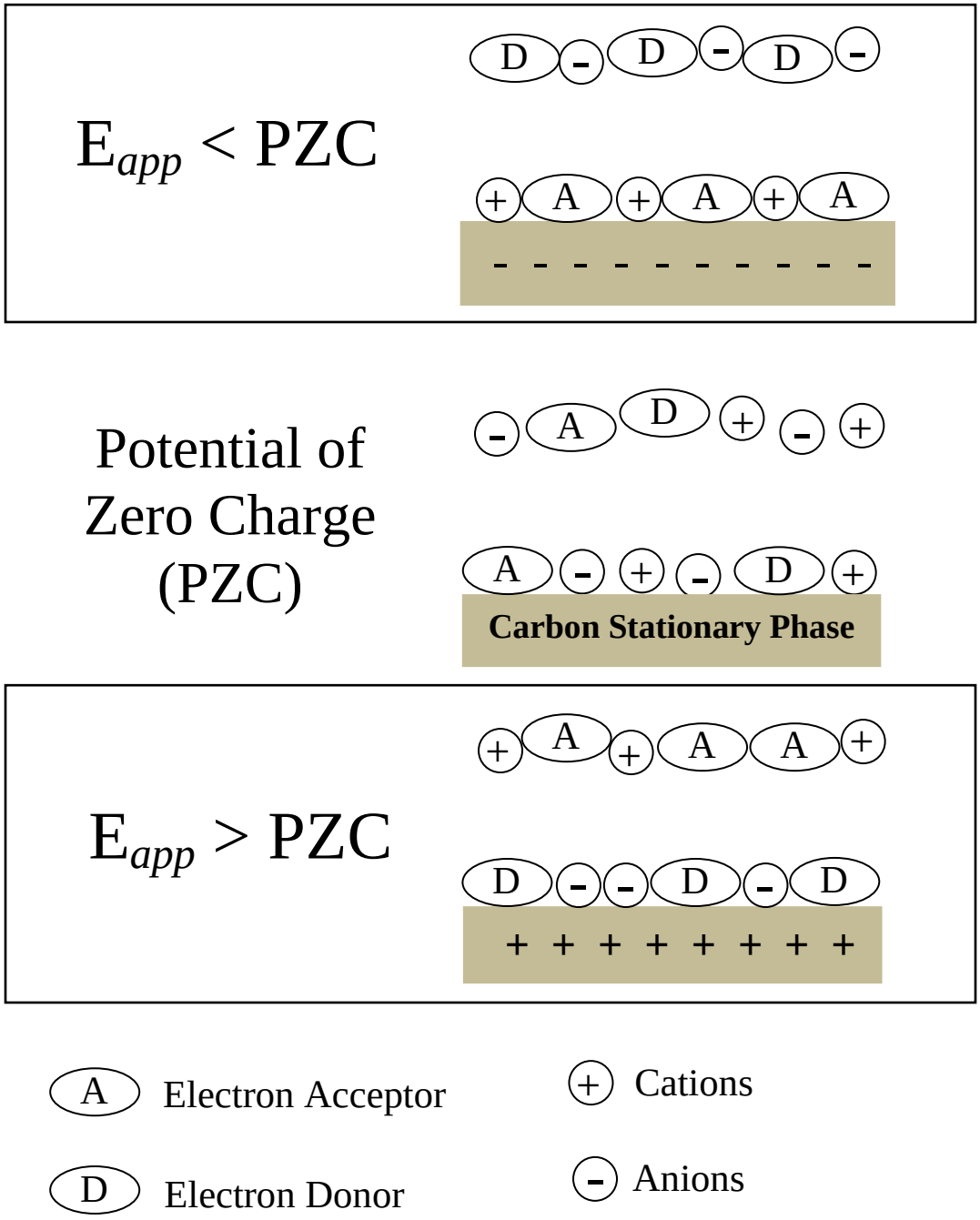

Figure 1-2. Schematic representation of the effects E_{app} has on the interactions with the stationary phase.

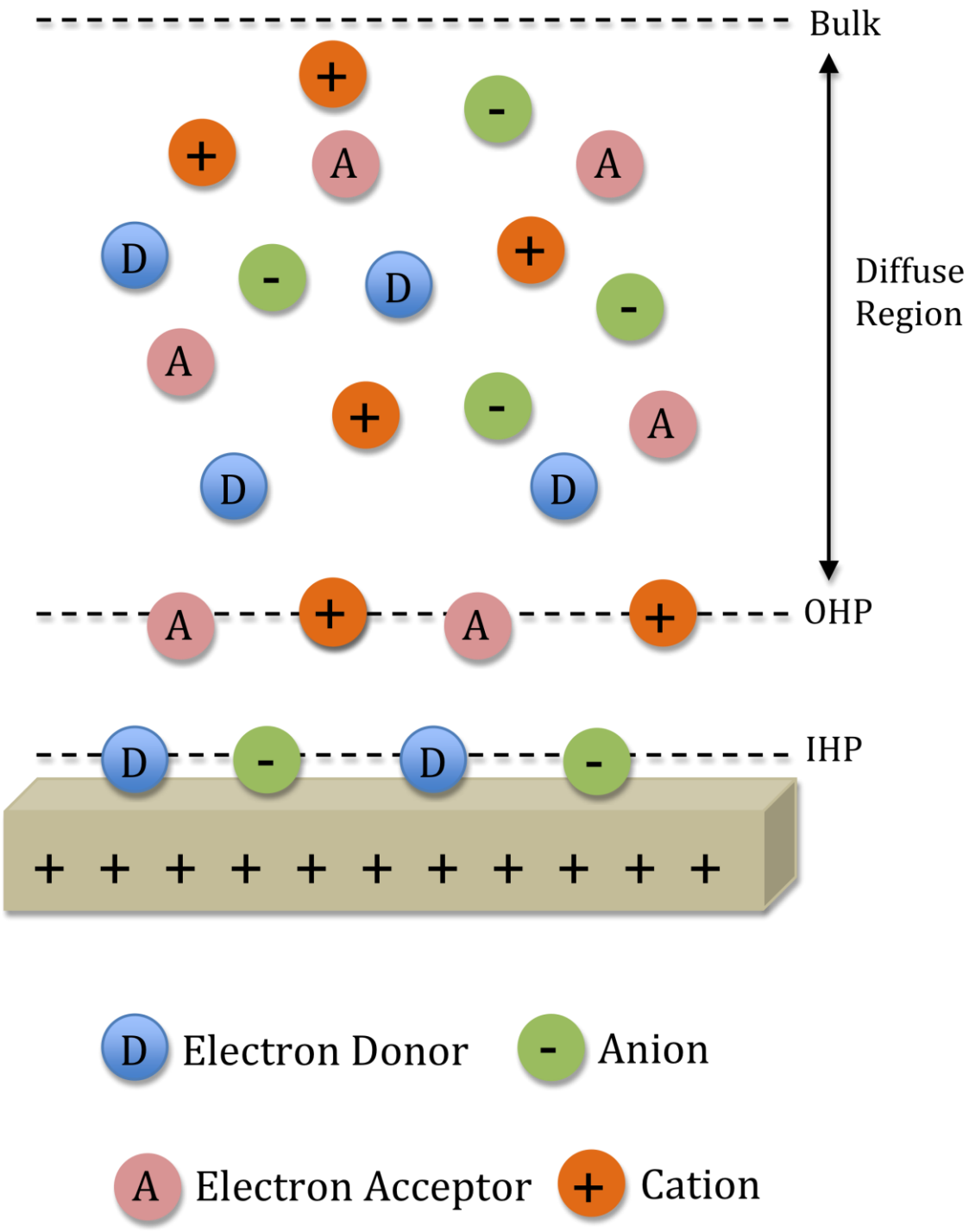

Figure 1-3. Schematic representation of the electrical double layer when E_{app} is positive of the PZC.

CHAPTER 2

EFFECTS OF ELUENT COMPOSITION ON RETENTION IN ELECTROCHEMICALLY MODULATED LIQUID CHROMATOGRAPHY

2.1 Abstract

The effect of changing the concentration of the organic modifier in the mobile phase on the electrosorption of aromatic sulfonates on porous graphitic carbon (PGC) was investigated by electrochemically modulated liquid chromatography (EMLC). EMLC uses a conductive stationary phase in that changing the electrical potential applied (E_{app}) to a conductive packing manipulates solute retention. The dependence of the capacity factor (ln k') on E_{app} with changing acetonitrile (ACN) concentration is linear below a 80:20 (*v*/*v* (H_2O/ACN)), but becomes nonlinear at higher ACN levels. The potential of zero charge (PZC), interfacial excess, and surface tension are evaluated as a basis to understand the interactions occurring at the surface. A detailed analysis reveals above 20% acetonitrile concentration in solution, the retention mechanism is dominated by the eluent composition rather than the electric field of the PGC.

2.2 Introduction

Electrochemically modulated liquid chromatography (EMLC) is a unique combination of high performance liquid chromatography (HPLC) and electrochemistry.[1]

This unique chromatographic technique employs a three-electrode electrochemical cell by using a conductive stationary phase (e.g., porous graphitic carbon (PGC),[1] glassy carbon (GC),[2,3] or boron-doped diamond particles (BDDP)[4]) that also functions as a working electrode. By altering the surface charge density through changes in the applied electrical potential (E_{app}) to the packing, solute retention is manipulated due to changes in the electrosorption process.[5] EMLC has been applied to the separation of a wide variety of mixtures, including aromatic sulfonates,[2,3,6] monosubstituted benzenes,[7] corticosteroids,[8] benzodiazepines,[9,10] enantiomers of hexobarbital and mephenytoin,[11] and inorganic ions.[12] The dependence of retention upon elevations in temperature has also been investigated.[13]

Other factors known to influence retention are the solvophobicity of the analyte and competition for adsorption sites on the PGC surface. For example, Horvath and coworkers[14] have applied solvophobic theory to reversed-phase HPLC as a means to describe the interactions between a solute and nonpolar, hydrocarbonaceous stationary phase. In that study, the retention of a large number of aromatic solutes (e.g., carboxylic acids, amino acids, and amines) was determined with water: methanol and water:acetonitrile mixed mobile phases. By examining the solvent properties through changes in solvent composition, the contribution of the solvophobic effect on retention was delineated. The analytes greatly solvated by the mobile phase or the solvophobic forces with the greatest influence on the capacity factor were found to be dependent on the surface tension in response to the mixed mobile phase. This dependence was viewed to result from organic solvent abruptly altering the structure of water. This solvent composition was shown to have an impact on the retention of the solutes. The

solvophobic effect entails interactions between the solute and solvent molecules or otherwise known as solvation. By examining the surface tension, the interactions occurring near the surface of the stationary phase was deduced.

A recent study incorporated the Gouy-Chapman diffuse double layer theory to understand competition between the analyte and the supporting electrolyte ions for adsorption sites on the stationary phase.[15] It was determined that retention is strongly affected by direct and indirect competition. Direct competition entails a difference in adsorption based on the identity of the electrolyte anion. The free energy of adsorption was calculated and was found to be different for different supporting electrolytes, signifying a competition for adsorption. Indirect competition occurs when the electrolyte concentration is manipulated, and is evident at higher electrolyte concentrations. Depending on the charge of the electrolyte and E_{app}, the adsorbed electrolyte creates a shield preventing electrostatic interactions from occurring between the analyte and the stationary phase.

Adsorption of aromatic sulfonates on PGC was found to span a range of interactions, including those based on dispersion, donor-acceptor strength, and solvophobicity. Dispersion interactions are attractive and nonspecific that occur between two polarizable species, where higher molecular weight solutes exhibit stronger interactions. Donor-acceptor interactions occur between the *n* and/or π electrons of the analyte and the delocalized π system of PGC. This interaction includes electrostatic and dipole-induced dipole interactions. The solvophobic effect arises from the solvation of an analyte with the mobile phase.[2] This paper investigates the effect of the concentration of the organic modifier, acetonitrile, has on the retention of aromatic sulfonates.

In this study, various compositions of H_2O:ACN mixtures were used in studying the electrosorption process of aromatic sulfonates on PGC. The data in this paper is interpreted based on three interactions: donor-acceptor, dispersion, and solvophobic. The previously described concepts concerning solvophobic theory and the competition for adsorption sites also aided in unraveling the data. To relate retention behavior to the changes in the organic modifier, the potential zero charge (PZC) was determined, along with several interfacial properties (e.g., interfacial excess and surface tension). The shifts in the values of the PZC and the change in the dependence of the capacity factor (ln *k'*) on E_{app} provide insight into the effects ACN has on the specific adsorption of the solutes.

2.2.1 Theory and Data Analysis

In earlier EMLC studies, we established the dependence of retention on E_{app} for aromatic sulfonates using monovalent (1:1) supporting electrolytes in a mixed solvent mobile phase 95:5 (*v*/*v* (H_2O/ACN)).[6] The retention of the solutes was found to increase as E_{app} became more positive, but to decrease as E_{app} moved more negative. Interactions responsible for causing this dependence were deduced from the plot of log *k'* vs E_{app}. A linear dependence was observed, indicating that the change in retention resulted from electrostatic interactions between the negatively charged sulfonate groups of the solutes and the PGC surface. That is, PGC has an excess positive surface charge density when E_{app} was positive of the PZC, resulting in an electrostatic attraction of the charged moieties of the analytes. When E_{app} was negative of the PZC, the PGC has an excess negative surface charge density, causing an electrostatic repulsion of the same moieties.

We recently reported on the use of EMLC as a means to determine the PZC for PGC.[16] This method correlated the retention dependence of aromatic suflonates with

respect to E_{app} as well as the identity and concentration of the supporting electrolyte. The potential at the point of convergence of an overlay of capacity-potential plots at different supporting electrolyte concentrations indicates that retention is independent of supporting electrolyte concentration, i.e., the PZC.

That study showed the PZC is dependent on the identity of the electrolyte anion and, to a lesser degree, the analyte. For the electrolyte, the greater its eluent strength, the more negative the PZC. We note that these observations have been predicted in a previous model on the roles the electrical double layer has on EMLC-based retention.[15] These and other factors will be taken into account in the subsequent data interpretation.

We have also applied the Gibbs adsorption equation to EMLC as a first principle assessment of thermodynamics that govern retention.[16] By assuming an ideally polarized electrode-solution interface and an absence of junction potentials, the Gibbs adsorption equation simplifies to the Gibbs-Duhem relationship, which is given in Equation 2-1.[17-19]

$$-d\gamma = q^M dE_{app} + \Sigma \Gamma_i d\mu_i \qquad (2\text{-}1)$$

In Equation 2-1, γ is the interfacial tension, q^M is the electrode charge, Γ_i is the interfacial excess, and μ_i is the chemical potential with *i* representing each of the ions in solution. When E_{app} remains constant, the Gibbs adsorption isotherm (Equation 2-2) can be used to determine the interfacial excess (Γ) for each component in the solution.

$$\left[\frac{-d\gamma}{d\mu_i}\right]_{Eapp} = \Gamma_i \qquad (2\text{-}2)$$

Γ_i is defined as the difference of species *i* in the interfacial region and bulk solution. The retention of these species provides information about the migration of the species from the mobile to stationary phase as defined in Equation 2-3.

$$k'_i = \frac{n_s}{n_m} \tag{2-3}$$

The capacity factor, k'_i, is defined as the ratio between the number of moles of species *i* on the stationary phase (n_s) to the number of moles in the mobile phase (n_m). To gain further information of the interfacial excess with the migration of species *i* from mobile to stationary phase, Equation 2-4 can be derived with *A* representing the surface area of the stationary phase.

$$\Gamma_i = \frac{1}{A}\left(n_s - n_m\right) \tag{2-4}$$

Equations 2-3 and 2-4 are then combined to form Equation 2-5, since the total concentration of the injected analyte is constant, and $n_{tot} = n_s + n_m$.

$$\Gamma_i = \frac{n_{tot}}{A}\left(\frac{k'_i - 1}{k'_i + 1}\right) \tag{2-5}$$

Equation 2-5 can be used to determine the change in $d\gamma$. Analysis of $d\gamma$ requires the molar approximation between $d\mu_i$ and the change in the mean activity coeffecient ($d\mu_i = 2RT$ d$\ln a$) and is determined from the slope of the plot of Γ_i versus 1/ln [SE], when SE represents the supporting electrolyte.

2.3 Experimental

2.3.1 Chemicals and Reagents

The stuctures of the analytes and their acronyms are listed in Figure 2-1. The analytes disodium 1,3-benzenedisulfonate, sodium benzenesulfonate, disodium 1,5-naphthalenedisulfonate, and disodium 2,6-napthalenedisulfonate were purchased from Aldrich (St. Louis, MO, USA). The supporting electrolyte, sodium hexafluorophosphate ($NaPF_6$), was aquired from Alfa Aesar (Ward Hill, MA, USA). Water and acetonitrile of high purity were obtained from EMD (Gibbstown, NJ, USA). All chemicals were used as received.

2.3.2 The EMLC Column

The design and construction of the column has been detailed elsewhere.[1,6] Briefly, a Nafion tubing (Perma Pure, Toms River, NJ, USA), which serves as a cation-exchange membrane, is inserted into a porous stainless steel cylinder (Mott Metallurgical). The column is slurry packed with PGC (Thermo Scientific), which serves as both a working electrode and stationary phase. A Ag/AgCl (saturated NaCl) reference electrode is placed inside an external reservoir that surrounds the porous stainless steel cylinder. All values of E_{app} are reported with respect to this reference electrode.

The experiments employed 5-μm diameter PGC particles as the stationary phase. PGC has been characterized by X-ray photoelectron spectroscopy (detection limit of ~0.200 atomic %) and found to have a very low level of surface oxygen-containing functional groups such as phenol, carboxylic acid, and quinone groups.[2] The manufacturer specifies a nominal pore diameter of ~ 250 Å with a porosity of ~80%.[20]

The surface area of PGC packed in the column is ca. 30.0 m^2, based on BET measurements (120 m^2/g)[16] and the amount of PGC packed in the column (~0.250 g).

2.3.3 Instrumentation

Chromatographic experiments were performed using an Agilent 1200 Series module equipped with a solvent cabinet, quaternary pumping system, autosampler, and a UV/Vis diode array detector. The module was interfaced to a Pentium IV 600 MHz computer with ChemStation software. The software is used for control of pump and injector parameters, set-up of sequences, and signal acquisition and data processing. The potential of the electrode was controlled using a high power potentiostat model 2055 (Amel Instruments, Milan, Italy).

2.3.4 Mode of Operation

The mobile phase composition was controlled by mixing water/acetonitrile (*v*/*v* (H_2O/ACN)) solution with a degasser on-line with the same H_2O:ACN solution that contained 120 mM $NaPF_6$. The mobile phase flow rate was 0.500 mL/min. The analytes were prepared at 50.0 μM concentration using water as the solvent. The nonretained peak for water was used for the determination of the dead time, t_0. The injection volume was 5.00 μL. The wavelength for detection was 220 nm. The separations were performed in triplicate at room temperature.

The mobile phase composition investigated ranged from 40.0 mM to 120 mM $NaPF_6$, increased by increments of 20.0 mM. After a change in E_{app} or the mobile phase, the system was allowed to reach a steady state (~30 min). All retention times, t_r, were

determined from the first statistical moment analysis of all chromatographic peaks.[21] The capacity factor, *k'*, was calculated according to Equation 2-6.

$$k' = \frac{t_r - t_o}{t_o} \qquad (2\text{-}6)$$

2.4 Results and Discussion

2.4.1 Effects of ACN on Retention

Representative effects of the amount of ACN (4-55%) in the mobile phase on the EMLC-based separation of the four-component mixture of aromatic sulfonates is shown in Figures 2-2 and 2-3 at an E_{app} of 0.000 V and -0.200 V and a $NaPF_6$ concentration of 100 mM. The data in Figure 2-2 presents the dependence of retention at low relative amounts of ACN (4, 6, and 8%; values given as percentage of ACN with respect to water) and values of E_{app} of 0.000 and -0.200 V. As is evident in Figure 2-2, retention decreases when E_{app} is changed from 0.000 to -0.200 V. This trend, which is followed by all four analytes for the tested values of E_{app} (+0.300 to -0.300 V in 0.150 V increments), is consistent with our earlier reports that correlate the dependence of retention with the change in the surface charge density on the electrode that is induced by changes in E_{app}.[1] Moreover, the data in Figure 2-2 shows that as the ACN concentration increases from 4 to 8%, the elution time reduces dramatically for all of the components of the mixture. For example, at an E_{app} of 0.000 V the total elution time of ~37 min at 4% ACN decreases to less than ~3 min at 8% ACN. This decrease, which translates to a reduction in elution time by a factor of 12.7, can be readily attributed to an increase in the solubility of these solutes as the dielectric constant of the mobile phase decreases with increases in ACN content.

Interestingly, as shown in Figure 2-3, the solutes undergo an increase in retention when the ACN concentration increases. These changes, however, are much more subtle in magnitude than found in Figure 2-2, and because of co-elution, injections of individual analytes were required to follow this trend. The data in Figure 2-3 present the effects of ACN on retention at an E_{app} of 0.000 V and a $NaPF_6$ concentration of 100 mM. When ACN increases above 8% in solution, the solute, 1,3-BDS undergoes an increase in retention. This same trend is observed for the solutes, 1,5-NDS and 2,6-NDS; however, the retention of 1,5-NDS increases in solutions containing greater than 15% ACN and the retention increases for 2,6-NDS in solutions greater than 35% ACN. The solute, BS, is no longer detectable in solutions containing 25% ACN and above and will need to be further investigated in future experiments.

The observed increase in retention has been reported for anilines in a water:acetonitrile mixed mobile phases containing $NaPF_6$ as the supporting electrolyte in reversed-phase HPLC.[22] In that work, the solutes elution time reached a maximum in a mobile phase composition of 20% ACN. This resulted from ACN forming a thick layer on the surface of the hydrophobic stationary phase. The adsorbed ACN molecules created a suitable media for adsorption of the PF_6^- anions by forming strong dispersive interactions with ACN π electrons. The solubility of the PF_6^- anions in this pseudo-stationary phase created an additional electrostatic component for retention. The addition of ACN not only created a pseudo-stationary phase, but also lowered the dielectric constant of the mobile phase, which increased the probability for ion pair formation.[22] Furthmore, PF_6^- is capable of forming ion pairs with the solute. The PF_6^- anion has a high degree of charge delocalization and a high polarizability. These properties enhance its

interaction with the solute, ultimately increasing retention. This interpretation is further examined in subsequent sections as a means for interpreting the trends in our data.

2.4.2 Potential Zero Charge

The PZC is determined for 1,3-BDS, BS, 1,5-NDS, and 2,6-NDS in $NaPF_6$ as shown in Table 2-1. The PZC decreases to more negative potentials as the ACN concentration decreases. Using the average PZC values for 1,3-BDS, there is a difference greater than 0.530 V when going from 3% to 20% ACN mixture. For BS and 1,5-NDS there is a difference greater than 0.700 V while for 2,6-NDS difference is greater than 0.650 V when going from 4% to 20% ACN in solution. It was previously described that as the eluent strength increases the PZC will shift to a more negative value; however, our data does not follow this previous observation.[16] One explanation is because at low ACN concentrations the solvated solute and the supporting electrolyte ions interact with the PGC predominantly through electrostatic interactions, but at higher ACN levels these interactions appear to no longer occur. The trends seen in retention and the PZC give a probable indication of a pseudo-stationary phase present in our system. These interactions and changes in the PZC are further evaluated in the capacity-potential plots.

Capacity-potential plots were examined to gain more insight into the interactions that may account for these changes in retention and the PZC. To further examine the impact of changes in ACN concentration, Figures 2-4 through 2-7 show the effect of changing the organic modifier concentration on the PZC for 1,5-NDS in a mobile phase with changes in both ACN and $NaPF_6$ concentrations. Note the linearity between ln k' and E_{app} at low ACN concentrations (i.e., 4 and 8% in Figures 2-4 and 2-5, respectively). This linearity further documents the role of electrostatic interactions on 1,5-NDS

retention as previously stated.[6] The E_{app} at which the plots for each supporting electrolyte concentration converge is determined to be the PZC. This is the potential in which retention is independent of the supporting electrolyte concentration; therefore, the electrostatic driving force for adsorption of the solutes on PGC is zero.[16] The PZC for 1,5-NDS in the mobile phase containing 4% ACN is determined to be -0.750 ± 0.255 V, but increases to a more negative value (-0.240 ± 0.037 V) in the mobile phase consisting of 8% ACN as shown in Figures 2-4 and 2-5.

Attempts to evaluate this trend by the point of convergence method for mobile phases containing a greater amount of ACN was hindered due to nonlinearity in the capacity-potential plots as shown in Figures 2-6 and 2-7. At ACN concentrations greater than 8% (35 and 55% ACN in Figures 2-6 and 2-7, respectively) the capacity-potential plots are markedly nonlinear, but parabolically shaped in a manner like the classic electrocapillary curve at mercury electrodes.[18] Thus, the maximum of the parabolic curve at ~0.000 V is the PZC.

A maximum in retention at 0.000 V at the different $NaPF_6$ concentrations (40.0 to 120 mM in 20.0 mM increments) is evident in Figures 2-6 and 2-7. At potentials positive of the PZC, the ACN molecules of the pseudo-stationary phase orients with the N atom towards the PGC where the nonbonding electrons of the N atom interact with the delocalized π system of the PGC. At potentials negative of the PZC, the ACN methyl group is orientated towards the electrode. At the PZC, the ACN molecules has no preferred orientation.[23,24] The PZC is the E_{app} at which the solute is capable of interacting with the PGC accounting for the maximum in retention. As E_{app} furthers from the PZC,

the solute is not able to form as strong of interactions with the PGC due to the thick adsorbed layer of ACN molecules shielding the solute from the surface potential field.

The two factors that influence retention in Figures 2-6 and 2-7 are: 1) ACN concentration and 2) $NaPF_6$ concentration. The change in retention, and ultimately the PZC, is due to the addition of ACN, which is attributed to the lowering of the dielectric constant of the mobile phase. This caused a breaking of the solvation shell, a H-bonded network of water molecules surrounding the solute.[22] It was recently found that the solute molecules are solvated by the water molecules in the bulk solution arising from the hydrophobic effect.[25] This addition of ACN molecules changed the dielectric constant, which in turn changed the polarization and interactions of the molecules in the mobile phase. The solute is then capable of forming strong interactions with the highly polarizable PF_6^- anion, which is adsorbed in the pseudo-stationary phase. An increase in $NaPF_6$ concentration caused an increased presence of PF_6^- anions in this pseudo-stationary phase, which created an additional electrostatic component that could alter adsorption. The solute was more capable of interacting with the PF_6^- anion due to its increased presence, which ultimately increased retention of the solute and altered the PZC.

The PZC shifts to more cathodic values as a result of this pseudo-stationary phase. The strong dispersive properties of ACN allows for a strong dispersive interaction with PF_6^-, with the electroneutrality of the system being reached at more cathodic values. The increase of the counterion, Na^+ cation, helps maintain electroneutrality of the system. At E_{app} greater than the PZC, the hydrated Na^+ cation is repelled by the electrode and can be

located in the diffuse layer of the EDL. At E_{app} less than the PZC, the hydrated Na^+ cation can be found in the outer Helmholtz plane of the EDL.[25]

2.4.3 Interfacial Excess

In order to further understand the interactions of the solute with PGC, the interfacial excess, Γ, was determined. The retention values of 50.0 μM 1,5-NDS in 100 mM $NaPF_6$ with varying concentrations of ACN were used to calculate Γ using Equation 2-5. The values for Γ were plotted against 1/ln [$NaPF_6$] in accordance with the Gibbs adsorption equation. The plot shown in Figure 2-8 is consistent with previous observations in that the slopes reflect the importance of electrostatic interactions.[16] A linear dependence is no longer observable when the ACN level is increased as shown in Figure 2-9 at 55% ACN indicating electrostatic interactions are no longer dominant at higher ACN levels.

As evident in Figure 2-9, Γ increases with increasing $NaPF_6$ concentration for E_{app} of +0.150, 0.000, and -0.150 V. The increase, however, is much weaker at +0.300 and -0.300 V. Γ is at a maximum for 120 mM $NaPF_6$ and at 0.000 V due to strong interactions between the PGC and the solute since the ACN molecules are randomly oriented on the surface and the PF_6^- anion is forming ion pairs with the solute as well as strong dispersive interactions with the ACN molecules. Retention at this potential and supporting electrolyte concentration is enhanced. As E_{app} moves farther from the PZC, retention decreases due to competition by adsorbed ACN.

In support of this claim, Γ is found to decrease as the ACN concentration increases as seen in Table 2-2. In 4% ACN, electrostatic interactions is the dominant interaction altering adsorption, which results in a larger value of Γ. As the ACN

concentration increases, adsorption is becoming dominated by the pseudo stationary-phase formed from ACN molecules and PF_6^- anions. This pseudo-stationary phase shields the solute from the surface electric field with the PF_6^- anion present in the pseudo-stationary phase contributing an electrostatic component capable of interacting with the solute.

2.4.4 Surface Tension

Surface tension, γ, was also studied to gain a better understanding of the surface interactions that may be occurring. The surface tension is calculated from a derived form of the Gibbs adsorption equation using the slopes from the Γ vs. 1/ln [$NaPF_6$] plot to calculate γ from Equation 2-2. An interesting feature is shown in Table 2-3 in that γ increases with increasing ACN concentration. As stated before, at 4% ACN, electrostatic interactions are the dominant interaction between the solute and the electrode. These electrostatic interactions cause competition between the electrolyte ions and the solute for adsorption sites on the PGC. As the ACN concentration is increased γ increases. This increase is caused by the thick layer of adsorbed ACN molecules on the surface, preventing the solute from easily absorbing to the surface of the PGC.

The ln *k'* as a function of ACN concentration is shown in Figure 2-10. All solutes exhibit a decrease in ln *k'* with increasing ACN levels, which then reach a minimum at 20% ACN, and then subsequently increases with increasing ACN in the mobile phase. This trend is in accordance with the increased retention observed with increasing ACN concentration.[26,27] At 20% ACN, the minimum in the curve represents a shift in the interactions occurring on the PGC. At ACN concentrations below 20%, the change in retention is dominated by electrostatic interactions. At ACN levels greater than 20%, the

retention is controlled by dispersive interactions between ACN molecules, PF_6^- anions, and the solute. The change in the polarization from the decrease in the dielectric constant of the mobile phase accounts for these strong dispersive interactions. The strong dispersive interactions between ACN molecules and PF_6^- anions created an additional electrostatic component to the retention mechanism. The lower dielectric constant increased the probability for ion pair formation, which also enhanced retention. These complex interactions are most likely to account for the increase in ln *k'* for the solutes.

2.5 Conclusions

This paper has demonstrated the effect the organic modifier, ACN, has on the electrosportion process of aromatic sulfonates in EMLC. By changing the organic modifier concentration, the solute retention can be manipulated along with its interaction with the PGC. At ACN concentrations greater than 20%, the electrosorption of the aromatic sulfonates changes from an electrostatic interaction to dispersive interactions between ACN molecules and the PF_6^- anion. In studying the interactions occurring in the system, there is no longer a linear dependence of ln *k'* on E_{app} when the ACN concentration is greater than 20% providing evidence of the lack of electrostatic interactions. The PZC was found to shift to more cathodic potentials with increasing ACN concentration due to ACN molecules adsorbing to the surface and forming strong dispersive interactions with the PF_6^- anion. The interfacial excess increased for E_{app} at the PZC, due to interactions with the solute and the PGC. The surface tension increased with increasing ACN concentration caused by the thick layer of adsorbed ACN molecules on the PGC surface. This effect on retention and the surface properties in EMLC will need to

be further studied by changing the identity of the supporting electrolyte and manipulating the temperature of the column.

2.6 Acknowledgement

Support for this project from the Utah Science Technology and Research Initiative (USTAR) is gratefully acknowledged.

2.7 References

1. Harnisch, J. A.; Porter, M. D. *Analyst* **2001**, *126*, 1841-1849.

2. Deinhammer, R. S.; Ting, E.-Y.; Porter, M. D. *Anal. Chem.* **1995**, *67*, 237-246.

3. Deinhammer, R. S.; Ting, E.-Y.; Porter, M. D. *J. Electroanal. Chem.* **1993**, *362*, 295-299.

4. Muna, G. W.; Swope, V. M.; Swain, G. M.; Porter, M. D. *J. Chromatogr. A* **2008**, *1210*, 154-159.

5. Nikitas, P. *J. Electroanal. Chem.* **2000**, *484*, 137-143.

6. Ting, E.-Y.; Porter, M. D. *Anal. Chem.* **1998**, *70*, 94-99.

7. Ting, E.-Y.; Porter, M. D. *J. Electroanal. Chem.* **1998**, *443*, 180-185.

8. Ting, E.-Y.; Porter, M. D. *Anal. Chem.* **1997**, *69*, 675-678.

9. Ting, E.-Y.; Porter, M. D. *J. Chromatogr. A* **1998**, *793*, 204-208.

10. Wang, S.; Porter, M. D. *J. Chromatogr. A* **1998**, *828*, 157-166.

11. Ho, M.; Wang, S.; Porter, M. D. *Anal. Chem.* **1998**, *70*, 4314-4319.

12. Ponton, L. M.; Porter, M. D. *J. Chromatogr. A* **2004**, *1059*, 103-109.

13. Ponton, L. M.; Porter, M. D. *Anal. Chem.* **2004**, *76*, 5823-5828.

14. Horvath, C.; Melander, W.; Molnar, I. *J. Chromatogr.* **1976**, *125*, 129-156.

15. Keller, D. W.; Ponton, L. M.; Porter, M. D. *J. Chromatogr. A* **2005**, *1089*, 72-81.

16. Keller, D. W.; Porter, M. D. *Anal. Chem.* **2005**, *77*, 7399-7407.

17. Devanathan, M. A. V.; Tilak, B. V. K. S. R. A. *Chem. Rev.* **1965**, *65*, 635.

18. Grahame, D. C. *Chem. Rev.* **1947**, *41*, 441-501.

19. Grahame, D. C.; Whitney, R. B. *J. Am. Chem. Soc.* **1942**, *64*, 1548-1552.

20. Knox, J. H.; Kaur, B. *J. Chromatogr.* **1986**, *352*, 3-25.

21. Foley, J. P.; Dorsey, J. G. *Anal. Chem.* **1983**, *55*, 730-737.

22. Kazakevich, Y.; LoBrutto, R. *HPLC for Pharmaceutical Scientists*; John Wiley & Sons, Inc.: New Jersey, 2007.

23. Baldelli, S.; Mailhot, G.; Ross, P.; Shen, Y.-R.; Somorjai, G. A. *J. Phys. Chem. B* **2001**, *105*, 654-662.

24. Faguy, P. W.; Fawcett, R. W.; Liu, G.; Motheo, A. J. *J. Electroanal. Chem.* **1992**, *339*, 339-353.

25. Pimienta, G. F. M.; Porter, M. D. *in preparation*.

26. Nahum, A.; Horvath, C. *J. Chromatogr.* **1981**, *203*, 53.

27. Nemeth-Kiss, V.; Forgacs, E.; Cserhati, T. *J. Chromatogr. A* **1997**, *776*, 147-152.

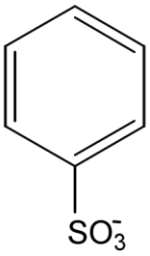

BS
Benzenesulfonate

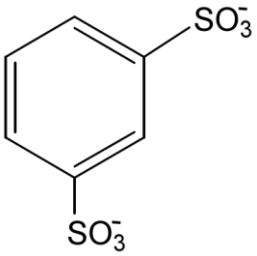

1,3-BDS
1,3-Benzenedisulfonate

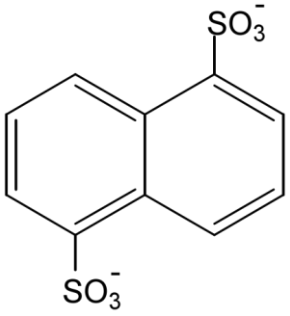

1,5-NDS
1,5-Naphthalenedisulfonate

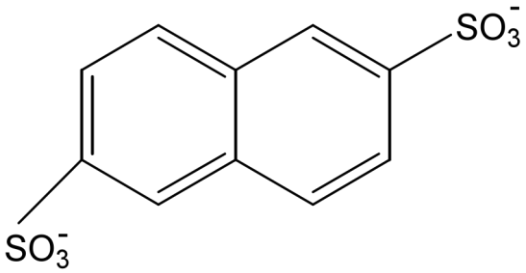

2,6-NDS
2,6-Naphthalenedisulfonate

Figure 2-1. Analyte structures and their acronyms.

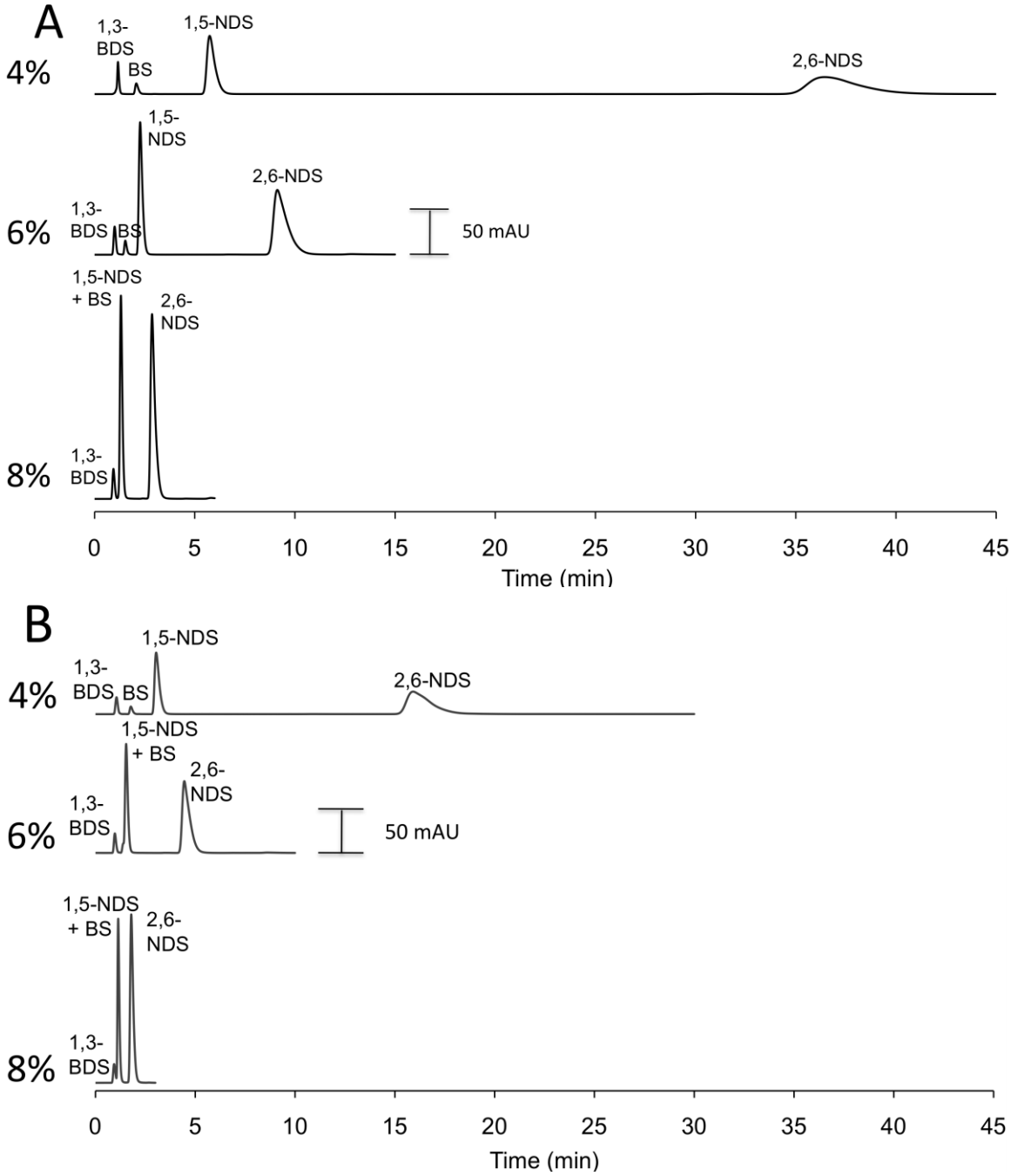

Figure 2-2. Chromatograms demonstrating the influence of ACN with a supporting electrolyte concentration ($NaPF_6$) of 100 mM at E_{app} of (A) 0.000 V and (B) -0.200 V vs Ag/AgCl/sat'd NaCl reference electrode. The mobile phase was a mixture of H_2O/ACN (4%, 6%, and 8% ACN), flowing at 0.500 mL/min. The analyte concentrations were 50.0 μM in H_2O.

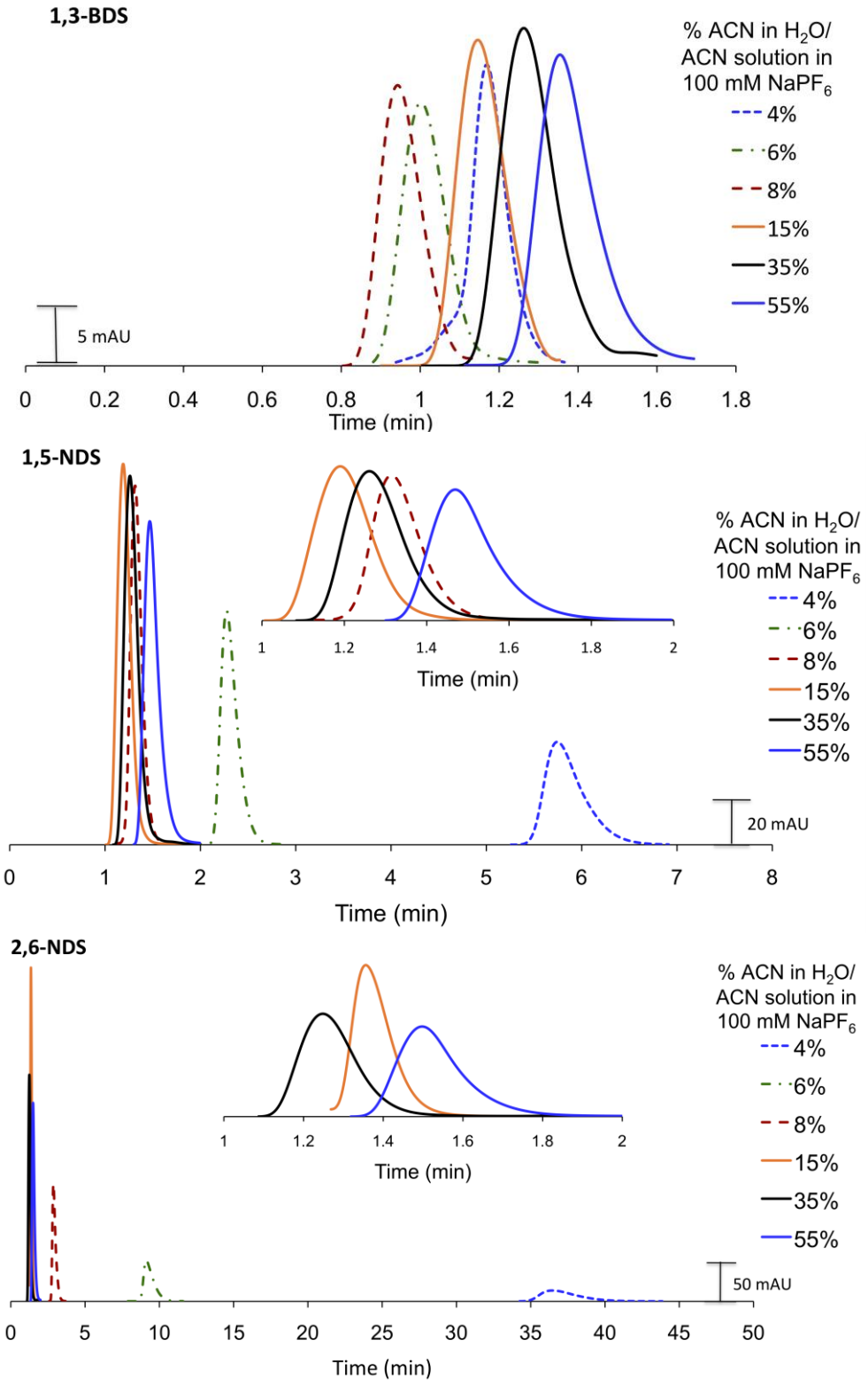

Figure 2-3. Dependence of the retention of 1,3-BDS, 1,5-NDS, and 2,6-NDS (all at 50.0 μM) in 100 mM $NaPF_6$ at E_{app} of 0.000 V. The mobile phase consists of varying H_2O:ACN mixtures at a flow rate of 0.500 mL/min. Figure insets are time-axis expansion in regions of comparable elution times.

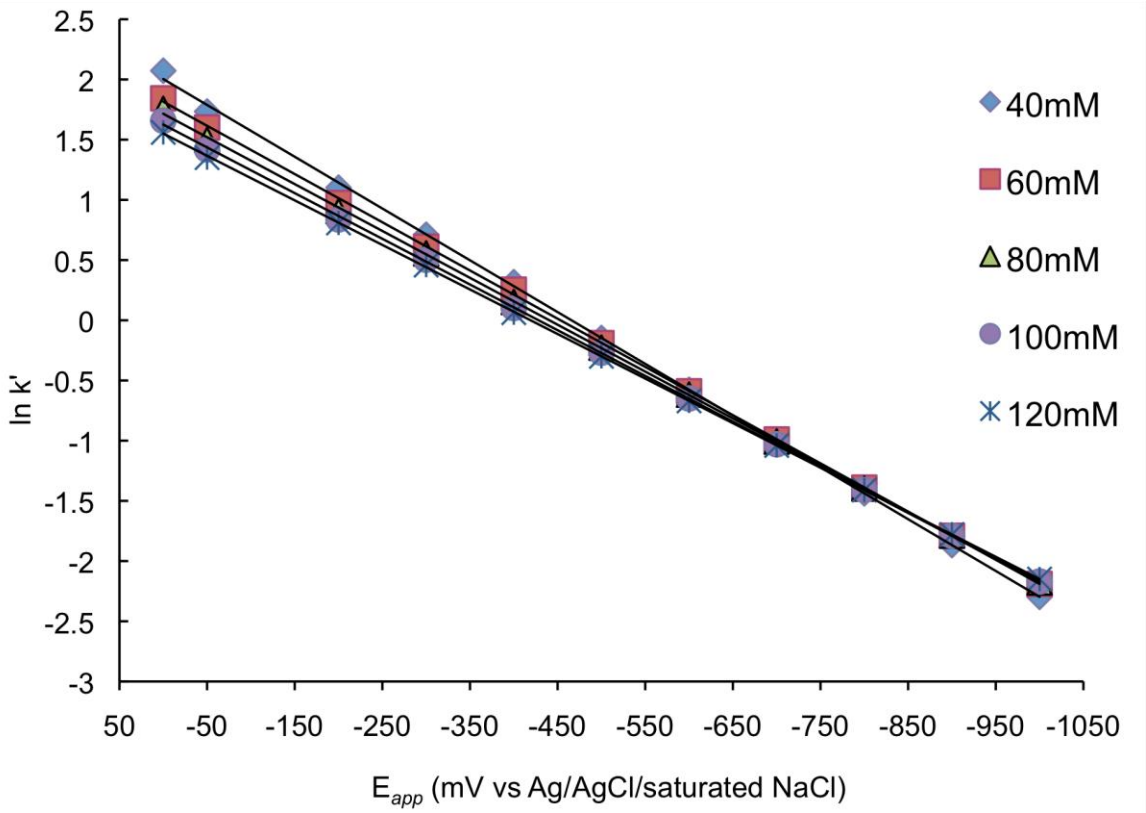

Figure 2-4. Plot of ln k' versus E_{app} for 1,5-NDS at multiple concentrations of $NaPF_6$ in 4% ACN. Each data point represents the average of three replicate injections with error bars on the order of the size of the points.

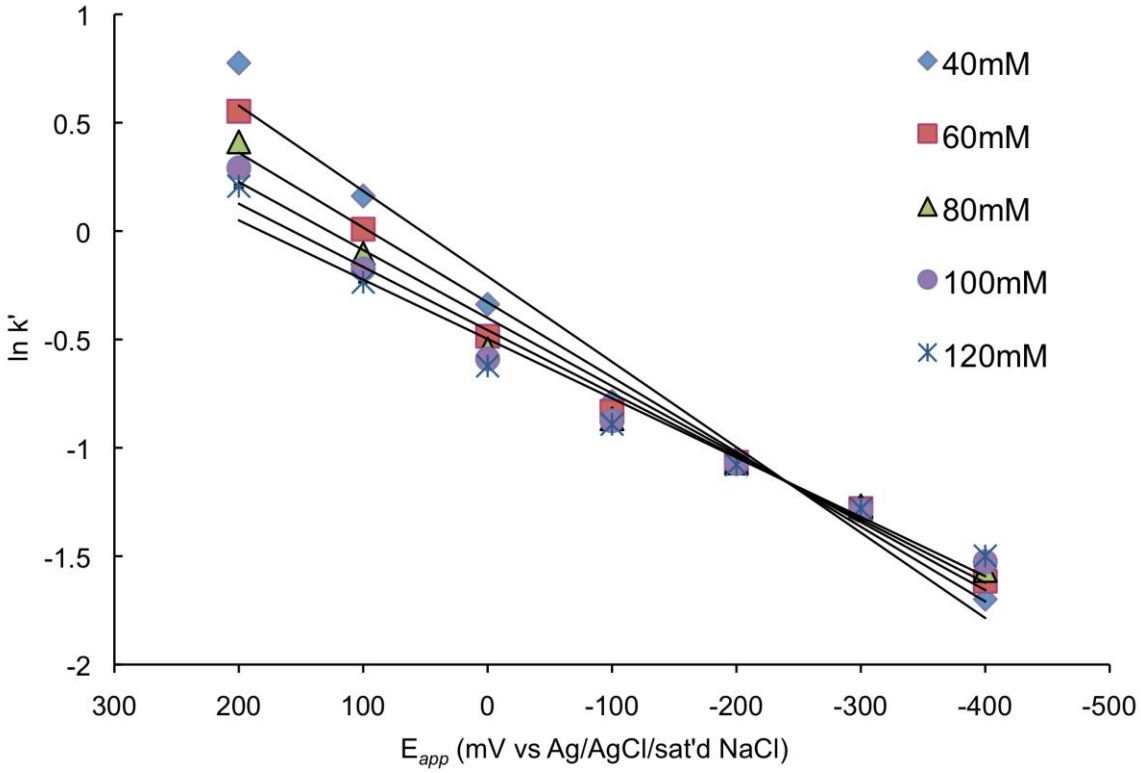

Figure 2-5. Plot of ln k' versus E_{app} for 1,5-NDS at multiple concentrations of $NaPF_6$ in 8% ACN. Each data point represents the average of three replicate injections with error bars on the order of the size of the points.

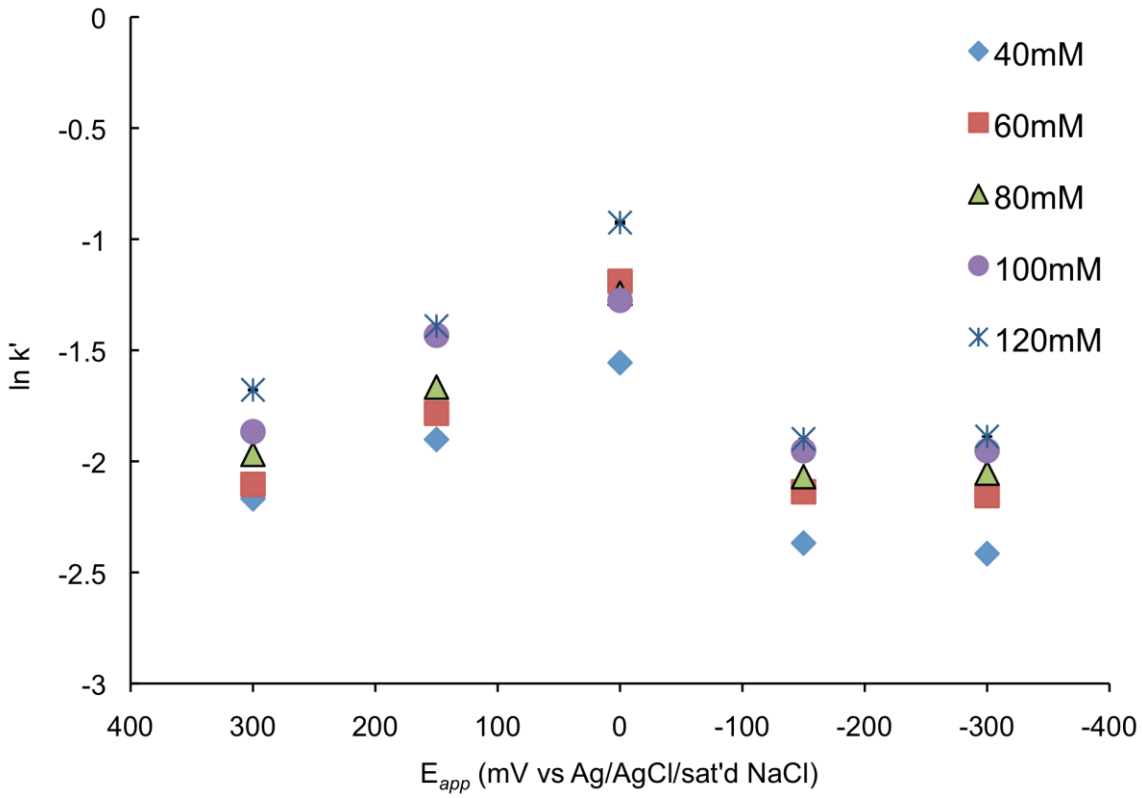

Figure 2-6. Plot of ln k' versus E_{app} for 1,5-NDS at different concentrations of $NaPF_6$ in 35% ACN. Each data point represents the average of three replicate injections with error bars on the order of the size of the points.

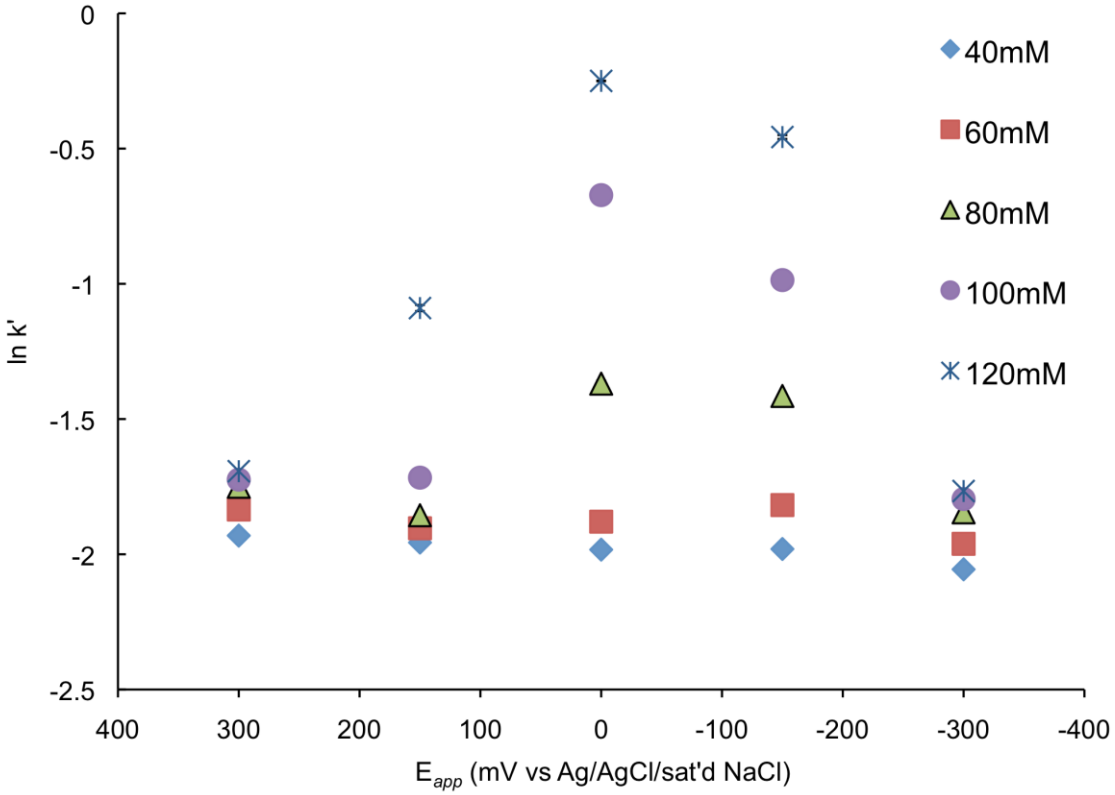

Figure 2-7. Plot of ln k' versus E_{app} for 1,5-NDS at different concentrations of $NaPF_6$ in 55% ACN. Each data point represents the average of three replicate injections with error bars on the order of the size of the points.

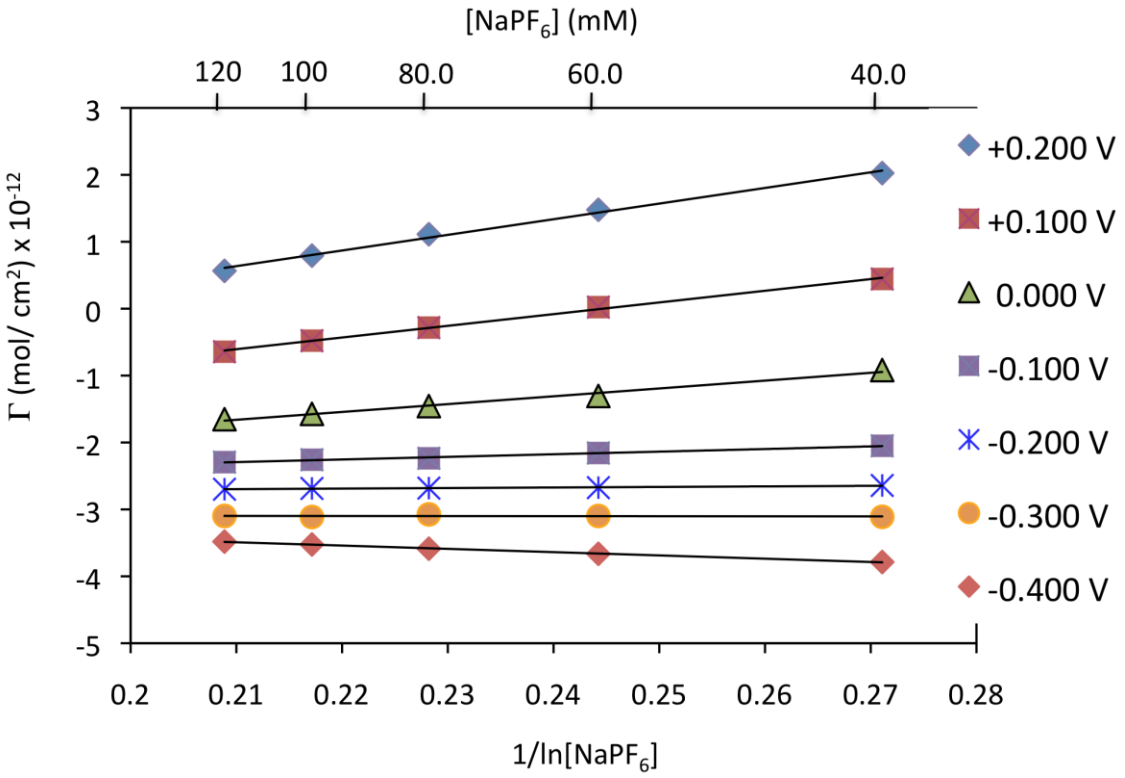

Figure 2-8. Interfacial excess plot for 1,5-NDS in 8% ACN at different E_{app} (versus Ag/AgCl/sat'd NaCl). Each data point represents the average of three replicate injections.

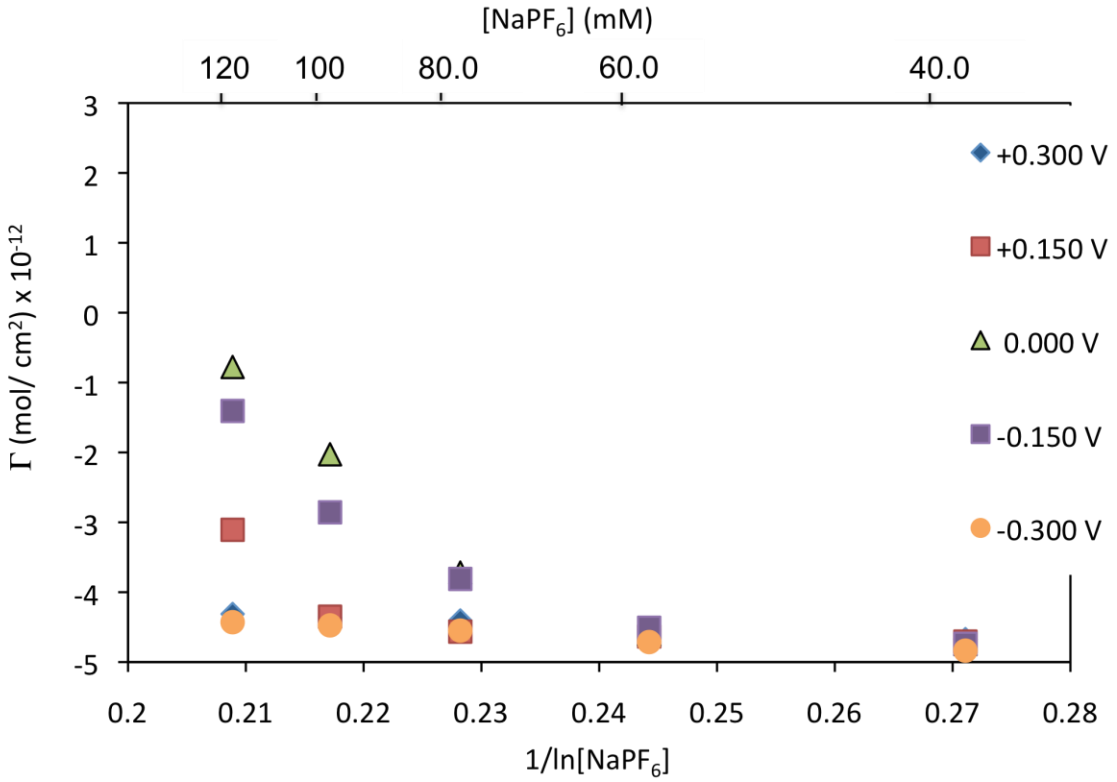

Figure 2-9. Interfacial excess plot for 1,5-NDS in 55% ACN at different E_{app} (versus Ag/AgCl/sat'd NaCl). Each data point represents the average of three replicate injections.

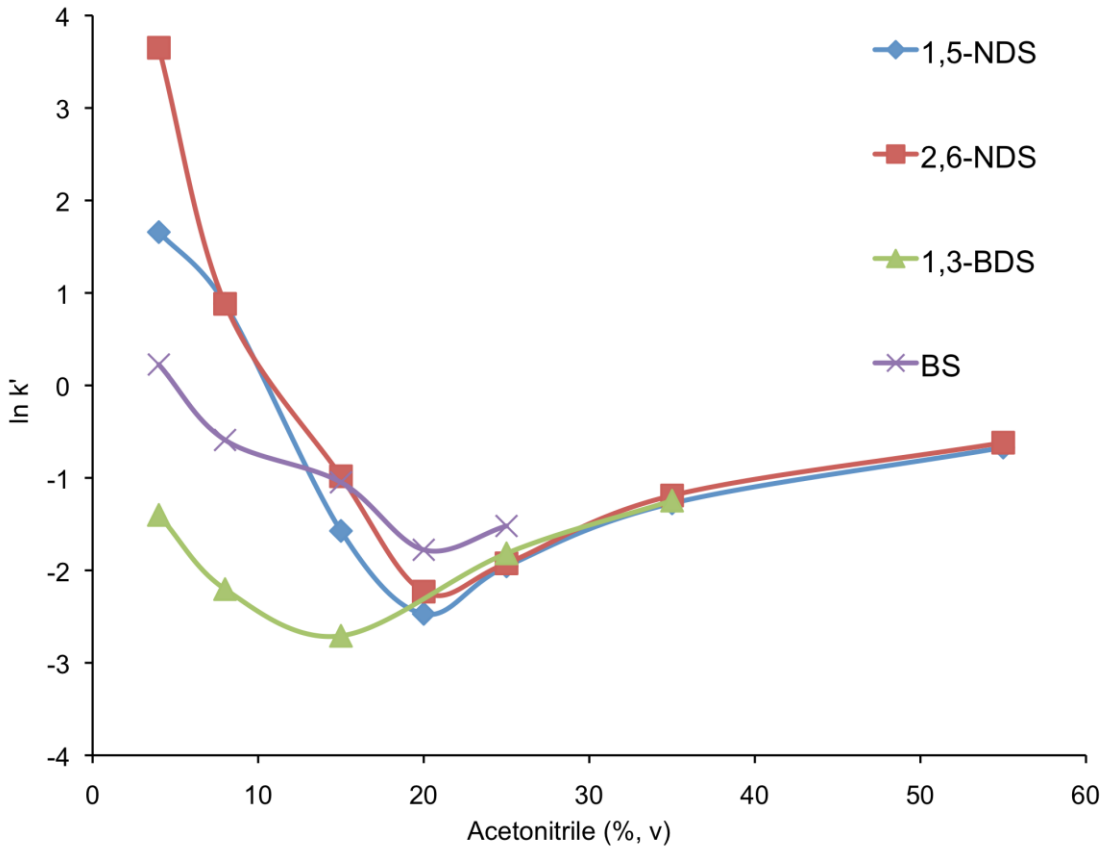

Figure 2-10. Retention as a function of ACN concentration in H_2O:ACN with 100 mM $NaPF_6$ as the mobile phase at E_{app} 0.000 V (versus Ag/AgCl/sat'd NaCl). The flow rate is 0.500 mL/min. The analytes were prepared to a concentration of 50.0 μM in H_2O. The lines are included as guides.

Table 2-1. Chromatographically determined values for the PZC of 1,3-BDS, BS, 1,5-NDS, and 2,6-NDS in H_2O:ACN mixtures with $NaPF_6$ as the supporting electrolyte. All values are in V vs Ag/AgCl/saturated NaCl reference electrode.

	H_2O:ACN						
Analyte	80:20	85:15	92:8	94:6	95:5	96:4	97:3
1,3-BDS	NA[a]	+0.345 ± 0.103	+0.200 ± 0.158	+0.070 ± 0.009	-0.025 ± 0.026	-0.100 ± 0.040	-0.130 ± 0.102
BS	+0.650 ± 0.061	+0.100 ± 0.075	-0.215 ± 0.067	-0.450 ± 0.110	-0.185 ± 0.050	-0.300 ± 0.077	NA[a]
1,5-NDS	+0.360 ± 0.013	+0.150 ± 0.075	-0.240 ± 0.037	-0.450 ± 0.080	-0.475 ± 0.115	-0.750 ± 0.255	NA[a]
2,6-NDS	+0.250 ± 0.001	-0.025 ± 0.016	-0.540 ± 0.176	-0.640 ± 0.170	-0.550 ± 0.122	NA[a]	NA[a]

[a] PZC that cannot be determined due to no point of convergence.

Table 2-2. Capacity Factors (k')[a] and interfacial excesses (Γ, $\times 10^{-12}$ mol/cm^2)[a] for a 5.00 μL injection of 50.0 μM 1,5-NDS in 100 mM $NaPF_6$ in 4, 8, 35, and 55% acetonitrile as a function of E_{app} (V vs Ag/AgCl/saturated NaCl reference electrode) and acetonitrile concentrations.

	H_2O:ACN							
	96:4		92:8		65:35		45:55	
E_{app} (V)	k'	Γ	k'	Γ	k'	Γ	k'	Γ
+ 0.300	—	—	—	—	0.154 ±0.001	-4.58	0.178 ±0.002	-4.36
+ 0.150	—	—	—	—	0.238 ±0.006	-3.84	0.179 ±0.001	-4.35
0.000	5.24 ±0.039	3.72	0.554 ±0.001	-1.57	0.279 ±0.005	-3.52	0.510 ±0.006	-2.02
- 0.150	—	—	—	—	0.142 ±0.002	-4.70	0.373 ±0.004	-2.85
- 0.200	2.31 ±0.005	2.17	0.342 ±0.002	-2.68	—	—	—	—
- 0.300	1.65 ±0.005	1.35	0.275 ±0.000	-3.11	0.142 ±0.002	-4.70	0.166 ±0.002	-4.47
- 0.400	1.10 ±0.003	0.279	0.217 ±0.000	-3.52	—	—	—	—

[a] Average values for three replicate injections.

Table 2-3. Values of surface tension for the analytes[a] as a function of change in ACN concentration in 100 mM $NaPF_6$ at E_{app} 0.000 V.

Analyte and % ACN	$d\gamma$ (J/cm^2) x 10^{-8}
<u>1,3-BDS</u>	
4%	-2.97
6%	-1.49
8%	2.97
15%	4.46
20%	-4.46
<u>BS</u>	
4%	-2.97
6%	-1.98
8%	1.98
15%	1.49
20%	2.97
<u>1,5-NDS</u>	
4%	-4.96
6%	-9.91
8%	-4.96
15%	3.47
20%	3.96
<u>2,6-NDS</u>	
4%	-0.991
6%	-3.47
8%	-9.91
15%	-0.446
20%	3.96

[a] Values show <1% RSD from the mean for the analytes.

CHAPTER 3

EXAMINATION OF MOBILE PHASE INTERACTIONS FOR ELECTROCHEMICALLY MODULATED LIQUID CHROMATOGRAPHY

3.1 Abstract

The impact of interactions in the bulk solution on the retention in electrochemically modulated liquid chromatography (EMLC) were investigated using attenuated total reflection FTIR spectroscopy (ATR-FTIRS). Herein, benzene is studied in solutions containing a mixture of water (H_2O) and acetonitrile (ACN) with lithium perchlorate ($LiClO_4$) as the supporting electrolyte. Benzene was found to interact with water and ACN molecules while also forming clusters with itself due to repulsive forces from water molecules. Ion association was found to occur between ClO_4^- anions and ACN molecules and the Li^+ cations and ClO_4^- anions, but not in the presence of water. Understanding the reactions occurring in the bulk solution will aid in developing a more fundamental mechanism behind the adsorption process. Future studies will provide information on reactions occurring when transferring from the mobile phase to the stationary phase.

3.2 Introduction

Retention mechanisms in liquid chromatography are dependent on interactions between the solute, stationary phase, and the mobile phase.[1-10] This paper focuses on interactions occurring in the mobile phase that change as the concentration of the organic modifier is altered.[7-10]

Ion association in the mobile phase and with the stationary phase can effect retention. Horvath and coworkers investigated ion-pair formation using a complexing agent, a strong electrolyte also referred to as a hetaeron, to enhance retention of oppositely charged solutes in ion-pair reversed-phase chromatography.[11] It was found that the solute and hetaeron formed a complex in the mobile phase that subsequently adsorbed to the stationary phase, and that the capacity factor, *k'*, was strongly dependent on the hetaeron concentration.

The hydrophobic effect[12] has also been used to account for retention mechanisms in chromatography. A recent study using electrochemically modulated liquid chromatography (EMLC) suggested that nonpolar, neutral aromatic solutes formed clusters in a polar solvent, which appear to disassemble when transferring from the mobile phase to the stationary phase and thus displacing adsorbed solvent molecules from the surface of the packing.[13] This increase in disorder resulted in an increase in the entropy of the system. Another laboratory took a thermodynamic approach in studying the hydrophobic effect in liquid chromatography.[14] In this case a nonpolar, neutral aromatic solute (e.g., toluene) was transferred from a nonpolar liquid, viz., poly(dimethylsiloxane) (PDMS) coated glass beads into a polar solvent at different

temperatures. The entropy and enthalpy of the system were found to be dependent on the temperature due to water structuring in close proximity of the nonpolar solutes. At higher temperatures, the water structure dissociated, increasing the disorder of the system, while the water structures appeared stable at room temperature. These studies provide an understanding of interactions that occur in the electrical double layer prior to solute adsorption.

In a different approach, infrared spectroscopy was used to investigate acetonitrile (ACN) in alkali-metal perchlorate solutions in order to explore electrolyte solvation. Fawcett and coworkers performed numerous studies of these interactions (e.g., ion-solvent and ion-ion) in solution.[15-21] By examining the CN stretching frequency of ACN, evidence was found for ion pairing between the cation and the lone pair electrons of the ACN nitrogen atom. The extent of these interactions was also shown to be dependent on the charge and the size of the cation. Ion pairing interactions were also found between the perchlorate anion and ACN. The T_d symmetry of ClO_4^- is lost in the presence of ACN due to interactions with the ACN methyl group. This ion pairing is associated with a split in the CH_3 rocking band of ACN.

In this paper, we examine the interactions occurring in solution when the composition is changed in order to gain an understanding of important factors that occur prior to the solute entering the electrical double layer in chromatographic retention by using attenuated total reflectance-Fourier transform infrared spectroscopy (ATR-FTIRS). More specifically, we examine a neutral aromatic solute (i.e., benzene) in solutions containing mixtures of water:acetonitrile (H_2O:ACN) and various concentrations of lithium perchlorate. This solution composition is similar to the mobile phase used in our

EMLC experiments, and an understanding of these interactions will aid in the development of retention mechanisms.

3.3 Experimental

Lithium perchlorate was purchased from Acros Organics. Benzene, high purity acetonitrile, and HPLC grade water were obtained from EMD. All reagents were used as received.

Infrared spectra were collected with a Nicolet 740 FTIR spectrometer equipped with a narrow-band HgCdTe detector cooled with liquid nitrogen. A circle cell (Spectra-Tech) with a ZnSe ATR crystal was used to perform the ATR-FTIRS experiments. A sample volume of 3 mL was injected into the cell. The cell was thoroughly rinsed with hexane, dichloromethane, ethanol, and finally methanol and dried with nitrogen gas between each experiment. The sample chamber was purged with $N_{2(g)}$ for 15 min before each spectra was collected. Spectra were collected by co-adding 512 scans at a resolution of 4 cm^{-1}. All spectra were referenced to an empty cell.

3.4 Results and Discussion

3.4.1 Change in the 3332 cm^{-1} OH Stretch of Water

The band with the largest change in shape is the OH stretch of water (3332 cm^{-1}) in the presence of ACN. Figure 3-1 shows the ATR-FTIR spectra of the OH stretch for water with 25% ACN containing $LiClO_4$ at 400 mM and 100 mM concentrations with and without 100 μM benzene. The strong band associated with the OH stretch for pure H_2O is visible at 3332 cm^{-1}. The much weaker bands at 2944 cm^{-1} and 3003 cm^{-1} are

assigned to the CH_3 stretching modes of ACN. As the amount of ACN increases (e.g., 60%), the OH stretch band broadens and decreases in strength when compared to pure H_2O as shown in Figure 3-1b. Upon inspection of the spectra for 25% and 60% ACN, no observable shift in the OH stretching band is evident at any of the $LiClO_4$ concentrations. However, a very subtle band shift of ~10 cm^{-1} occurs with 100 μM benzene in solution.

This shift is attributed to interactions between water and benzene. Benzene is hydrophobic and when placed in an aqueous environment, it will form clusters and hydrogen-bonds with water.[22-29] As developed from various molecular dynamics and force field calculations, the formation of hydrogen-bonds may be due to the quadrupole moment of benzene (Θ = -29.0 x 10^{-40} C m^2).[30] Benzene has a negative partial charge on its face and a positive partial charge around its edges.[25] The water molecules position themselves above the benzene molecule to form hydrogen-π interactions. The benzene molecules will also form clusters through π-π interactions while the water molecules form a hydration shell through a hydrogen-bonded network. Indeed, for solutions containing greater than 100 μM of benzene, there is a visible phase separation. The phase at the surface of the cell contains mostly benzene and ACN while the layer towards the outside of the cell is mostly composed of water and ACN.

3.4.2 The 1480 cm^{-1} C=C Stretch Band

ATR-FTIR spectra for the solutions containing 1.00 M benzene in 100 mM and 400 mM $LiClO_4$, with 100, 60, and 25% ACN are shown in Figure 3-2. The band at 1480 cm^{-1} is assigned to the C=C stretch of benzene. This band increases in absorbance for solutions composed of 25% ACN compared to solutions containing 100% or 60% ACN.

The order of greatest absorbance of the solutions are 25%>100%>60% ACN. This is, at first, an unexpected result.

The change in absorbance as a function of H_2O:ACN concentration points to complex interactions between benzene, water, and ACN. These include benzene molecules interacting with other benzene molecules and with water. Benzene is a hydrophobic molecule so when placed in water, benzene has a "repulsive" interaction with water but an "attractive" interaction with other benzene molecules. This attractive interaction leads to the formation of benzene clusters, which leads to phase separation. These clusters are located near the surface of the ATR cell allowing for a stronger absorbance in the 1480 cm^{-1} C=C stretch of benzene. In 60% ACN, benzene molecules appear to form smaller clusters. This phase separation appears to be the same for this mixture having the lowest absorbance for the 1480 cm^{-1} C=C stretch of benzene. In 100% ACN, benzene does not phase separate.

Benzene-water interactions are also suggested by a shift in the 1814 cm^{-1} overtone band of benzene in Figure 3-3. This band shifts 10 cm^{-1} in higher energy in a H_2O:ACN mixture. There is no observable shift or change in the band shape when the $LiClO_4$ concentration is changed. The intensity of absorbance of this band, however, follows the same trend seen in the 1480 cm^{-1} C=C stretching band of benzene (Figure 3-2).

3.4.3 Shift in the 1814 cm^{-1} Overtone Band of Benzene

ATR-FTIR spectra of the 1814 cm^{-1} overtone band for benzene is shown in Figure 3-3. The band shifts to higher energy by 13 cm^{-1} in ACN. ACN is, comparatively, a highly polar solvent with a large dipole moment.[31] This shift is due to interactions between benzene and ACN molecules. A previous study reported a dipole-induced dipole

interaction between ACN and benzene.[32] This interaction was found to occur in two ways: 1) between the benzene π system and the ACN methyl group and 2) between the H atoms of benzene and the lone pair electrons on the N atom of ACN.[29] In ACN rich solutions, benzene molecules favor interaction with ACN, but these interactions are much weaker in water rich solutions since benzene is a hydrophobic molecule in a hydrophilic solution.[31] This effect is shown by the 10 cm^{-1} shift when water is added to the mixture.

3.4.4 Intermolecular Interactions Occurring with Li^+ Cation

In previous work,[15-21] interactions between ACN and perchlorate were used to explain the results found herein. ATR-FTIR spectra of the CC stretch region and the CN stretch region of ACN are shown in Figure 3-4. The band located at 918 cm^{-1} confirms the identity of the CC stretch of ACN in Figure 3-4a. When no water is present, a band appears at 931 cm^{-1}. Fawcett and coworkers attributed this to coordination between the Li^+ cation and the CC stretch of ACN. In Figure 3-4b, the two bands at 2253 cm^{-1} and 2293 cm^{-1} are assigned to the CN stretch and the combination band for the CC stretch and the CH_3 deformation modes of ACN, respectively. When water is absent, a new band appears at 2275 cm^{-1} and 2305 cm^{-1}, indicating solvation of the Li^+ cation by ACN. The solvation number has previously been reported to be 2.08 ± 0.02.[21] When water is added to the system, these bands disappear, indicating there is no longer any observable coordination or solvation of the Li^+ cation with acetonitrile molecules.

3.4.5 Intermolecular Interactions Occurring with the ClO_4^- Anion

The ClO_4^- anion interactions in H_2O:ACN mixtures are interpreted similar to that of the Li^+ cations. ATR-FTIR spectra of the CH_3 rock band of ACN are shown in Figure

3-5. The 1039 cm^{-1} rock band for pure ACN splits into 1039 cm^{-1} and 1101 cm^{-1} in the presence of $LiClO_4$. Previous studies by Fawcett and coworkers attributed the 1101 cm^{-1} band to coordination between the ClO_4^- anion and ACN molecules. In Figure 3-5a, a new band appears at 1131 cm^{-1}, which is assigned to ClO_4^- anions forming aggregates with Li^+ cations. As the $LiClO_4$ concentration increases, the coordination between the Li^+ cation and the ClO_4^- anion increases as well. When water is added to the system as shown in Figure 3-5b, the band at 1131 cm^{-1} disappears and the band at 1101 cm^{-1} is still present indicating the ClO_4^- anions coordinates with ACN molecules but does not aggregate with the Li^+ cations since the Li^+ cations are being solvated by water molecules.

3.5 Conclusions

This study has shed light on the interactions that may be occurring in the bulk solution during our EMLC experiments. First, benzene and water molecules form hydrogen-bonds when benzene is present at low concentrations (Figure 3-1). At concentrations greater than 100 μM benzene, hydrophobic forces dominate the system. The attraction between benzene molecules increases and clusters form. These clusters are enclosed by a hydration shell formed by a hydrogen-bonded network of water molecules. This repulsive interaction results in a phase separation affecting the absorbance of the 1480 cm^{-1} CC stretch benzene band in the spectra (Figure 3-2).

Benzene was found to interact with ACN molecules as indicated by the 1814 cm^{-1} overtone benzene band. Further studies will need to be performed in order to determine how ACN and benzene are coordinated in solution. Interesting, it was found the $LiClO_4$ had little effect on benzene since there is no shift in any benzene band when the $LiClO_4$

concentration is changed indicating there is no evidence of interaction occurring between benzene molecules and $LiClO_4$ ions.

Other interactions include ion association involving the $LiClO_4$ ions. For the case of neat ACN, Li^+ cations are solvated by ACN molecules (2275 cm^{-1} and 2305 cm^{-1}) and coordinates to ACN (931 cm^{-1}) and ClO_4^- anions (1131 cm^{-1}); however, these interactions are no longer visible when water is added to solution. The Li^+ cation is instead solvated by the water molecules. The ClO_4^- anion coordinates to ACN in 100% ACN and in H_2O:ACN mixtures (1101 cm^{-1}). These interactions may play a role in the retention time of analytes and need to be monitored when conducting future investigations when formulating a retention mechanism. In the future, we plan to study the effect of applied potential on the adsorption and interaction of solute and stationary phase, solute and mobile phase, and the mobile and stationary phase.

3.6 Acknowledgement

Support for this project from the Utah Science Technology and Research Initiative (USTAR) is gratefully acknowledged.

3.7 References

1. Hanai, T. *J. Chromatogr. A* **2003**, *989*, 183-196.

2. Kriz, J.; Adamcova, E.; Knox, J. H.; Hora, J. *J. Chromatogr. A* **1994**, *663*, 151-161.

3. Lepont, C.; Gunatillaka, A. D.; Poole, C. F. *Analyst* **2001**, *126*, 1318-1325.

4. Melander, W. R.; Horvath, C. *Chromatographia* **1984**, *18*, 353-361.

5. Schmickler, W. *Chem. Rev.* **1996**, *96*, 3177-3200.

6. Vailaya, A.; Horvath, C. *J. Chromatogr. A* **1998**, *829*, 1-27.

7. Wang, A.; Tan, L. C.; Carr, P. W. *J. Chromatogr. A* **1999**, *848*, 21-37.

8. Snyder, L. R. *Principles of Adsorption Chromatography*; Marcel Dekker Inc: New York, 1968.

9. Snyder, L. R.; Dolan, J. W. *High-Performance Gradient Elution: The Practical Application of the Linear-Solvent-Strength Model*; John Wiley & Sons, Inc.: New Jersey, 2007.

10. Wang, A.; Carr, P. W. *J. Chromatogr. A* **2002**, *965*, 3-23.

11. Horvath, C.; Melander, W.; Molnar, I.; Molnar, P. *Anal. Chem.* **1977**, *49*, 2295-2305.

12. Ben-Naim, A. *Hydrophobic Interactions*; Plenum Press: New York, 1980.

13. Pimienta, G. F. M.; Porter, M. D. *in preparation*.

14. Silveston, R.; Kronberg, B. *J. Phys. Chem.* **1989**, *93*, 6241-6246.

15. Faguy, P. W.; Fawcett, W. R.; Patrick, D. L. *J. Chem. Soc., Faraday Trans.* **1991**, *87*, 2961-2965.

16. Fawcett, W. R. *J.Phys. Chem.* **1993**, *97*, 9540-9546.

17. Fawcett, W. R.; Liu, G. *J. Phys. Chem.* **1992**, *96*, 4231-4236.

18. Fawcett, W. R.; Liu, G.; Faguy, P. W.; Foss Jr., C. A.; Motheo, A. J. *J. Chem. Soc., Faraday Trans.* **1993**, *89*, 811-816.

19. Fawcett, W. R.; Liu, G.; Kessler, T. E. *J. Phys. Chem.* **1993**, *97*, 9293-9298.

20. Fawcett, W. R.; Liu, G.; Kloss, A. A. *J. Chem. Soc., Faraday Trans.* **1994**, *90*, 2697-2701.

21. Loring, J. S.; Fawcett, W. R. *J. Phys. Chem. A* **1999**, *103*, 3608-3617.

22. Allesch, M.; Schwegler, E.; Galli, G. *J. Phys. Chem. B* **2007**, *111*, 1081-1089.

23. Feller, D. *J. Phys. Chem. A* **1999**, *103*, 7558-7561.

24. Lee, S. H.; Kim, J. H.; Chu, I.; Song, J. K. *Phys. Chem. Chem. Phys.* **2009**, *11*, 9468-9473.

25. Lopes, P. E. M.; Lamoureux, G.; Roux, B.; MacKerell, A. D. J. *J. Phys. Chem. B* **2007**, *111*, 2873-2885.

26. Nakahara, M.; Wakai, C.; Yoshimoto, Y.; Matubayasi, N. *J. Phys. Chem.* **1996**, *100*, 1345-1349.

27. Slipchenko, L. V.; Gordon, M. S. *J. Phys. Chem. A* **2009**, *113*, 2092-2102.

28. Suzuki, S.; Green, P. G.; Bumgarner, R. E.; Dasgupta, S.; Goddard III, W. A.; Blake, G. A. *Science* **1992**, *257*, 942-945.

29. Ugozzoli, F.; Arduini, A.; Massera, C.; Pochini, A.; Secchi, A. *New J. Chem.* **2002**, *26*, 1718-1723.

30. Hunter, C. A.; Lawson, K. R.; Perkins, J.; Urch, C. J. *J. Chem. Soc., Perkin Trans.* **2001**, *2*, 651-669.

31. Luther, B. M.; Kimmel, J. R.; Levinger, N. E. *J. Chem. Phys.* **2002**, *116*, 3370-3377.

32. Yadava, R. R.; Yadava, S. S. *Rev. Roum. Chim.* **1991**, *36*, 1259-1262.

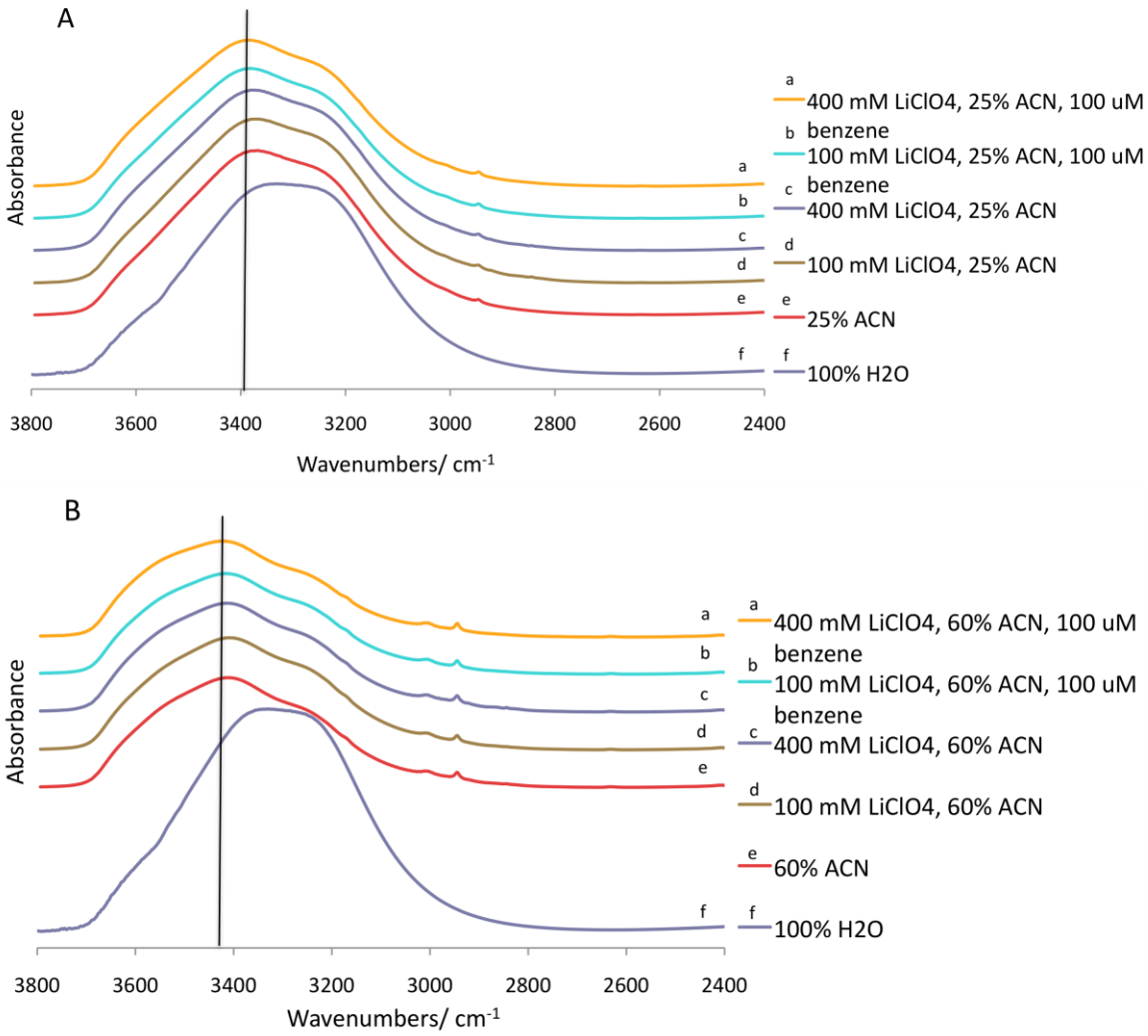

Figure 3-1. ATR-FTIR spectra of the OH stretching region of H_2O (3800-2400 cm^{-1}) for solutions containing 25% ACN (A) and 60% ACN (B). The solution compositions are as follows: (a) 400 mM $LiClO_4$ in ACN with 100 μM benzene, (b) 100 mM $LiClO_4$ in ACN with 100 μM benzene, (c) 400 mM $LiClO_4$ in ACN, (d) 100 mM $LiClO_4$ in ACN, (e) H_2O:ACN mixture and (f) neat H_2O.The spectra have been offset for clarity. The lines are a guide for viewing the subtle shifts in the OH stretch.

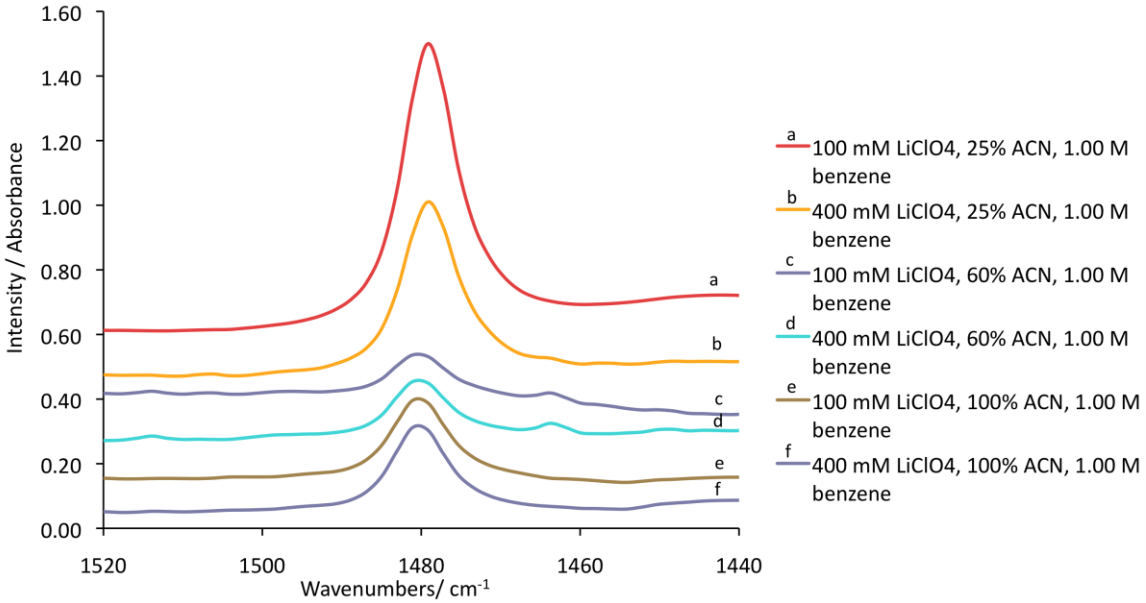

Figure 3-2. ATR-FTIR spectra of the CC stretch region (1520-1440 cm^{-1}) for benzene containing (a) 100 mM $LiClO_4$ in 25% ACN with 1.00 M benzene, (b) 400 mM $LiClO_4$ in 25% ACN with 1.00 M benzene, (c) 100 mM $LiClO_4$ in 60% ACN with 1.00 M benzene, (d) 400 mM $LiClO_4$ in 60% ACN with 1.00 M benzene, (e) 100 mM $LiClO_4$ in 100% ACN with 1.00 M benzene and (f) 400 mM $LiClO_4$ in 100% ACN with 1.00 M benzene. The spectra have been offset for clarity.

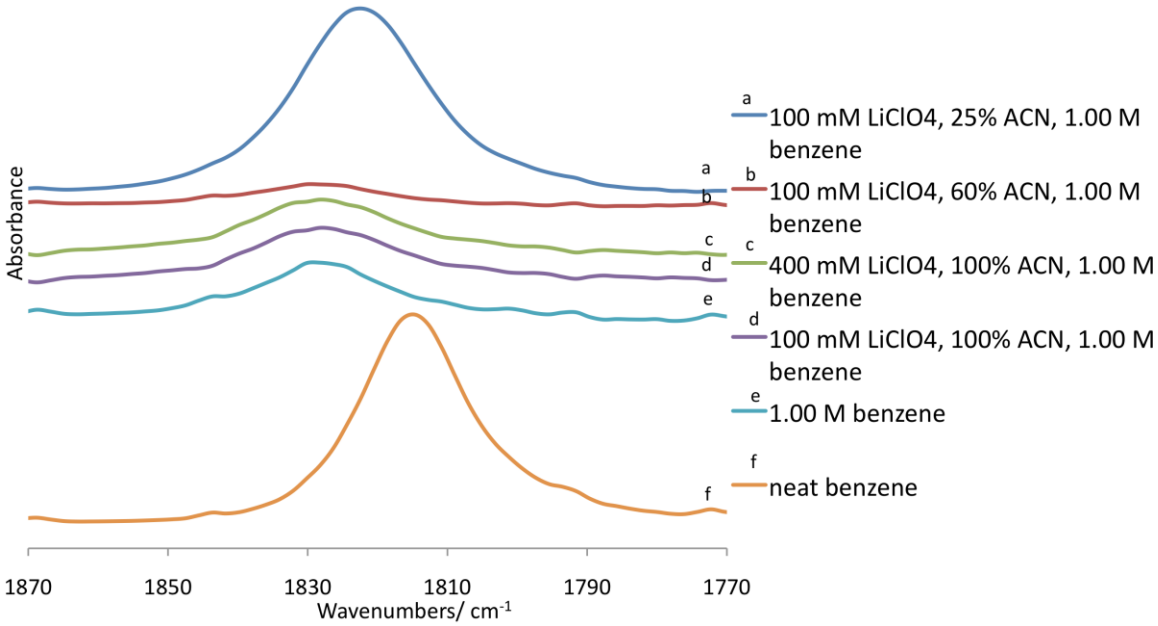

Figure 3-3. ATR-FTIR spectra of the overtone region (1870-1770 cm^{-1}) for benzene in solutions containing (a) 100 mM $LiClO_4$ in 60% ACN with 1.0 M benzene, (b) 100 mM $LiClO_4$ in 25% ACN with 1.0 M benzene, (c) 400 mM $LiClO_4$ in 100% ACN with 1.0 M benzene, (d) 100 mM $LiClO_4$ in 100% ACN with 1.0 M benzene, (e) 1.0 M benzene in ACN and (f) neat benzene. The spectra have been offset for clarity.

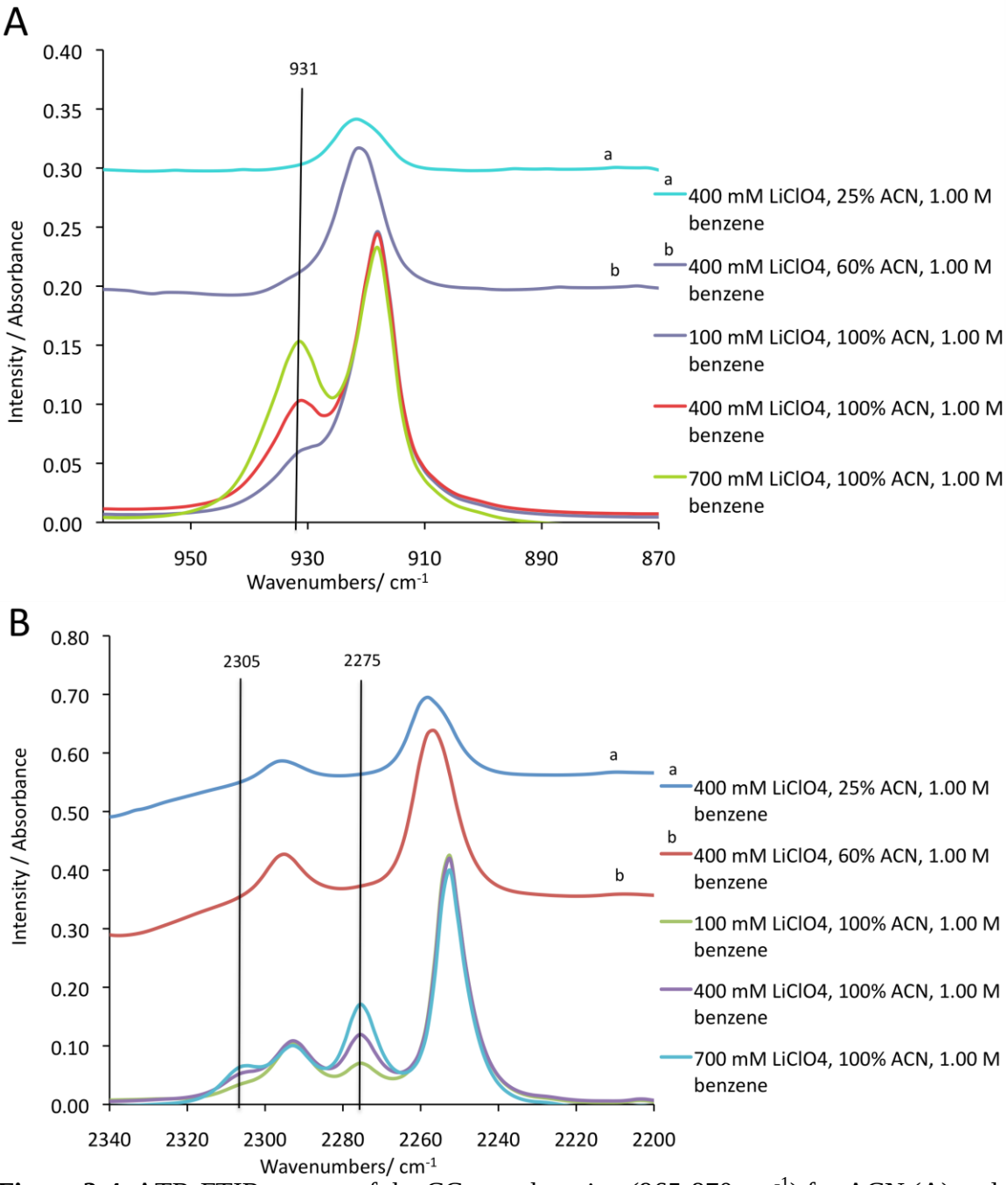

Figure 3-4. ATR-FTIR spectra of the CC stretch region (965-870 cm^{-1}) for ACN (A) and of the CN stretch region (2340-2200 cm^{-1}) for ACN (B). The solutions contain (a) 400 mM $LiClO_4$ in 25% ACN with 1.0 M benzene, (b) 400 mM $LiClO_4$ in 60% ACN with 1.0 M benzene and an overlay of 100 mM, 400 mM, and 700 mM $LiClO_4$ in 100% ACN with 1.0 M benzene. The spectra in (a) for 100% ACN solutions have been normalized to the 918 cm^{-1} peak for 700 mM $LiClO_4$ 100% ACN. The solutions containing water (a and b) were offset for clarity.

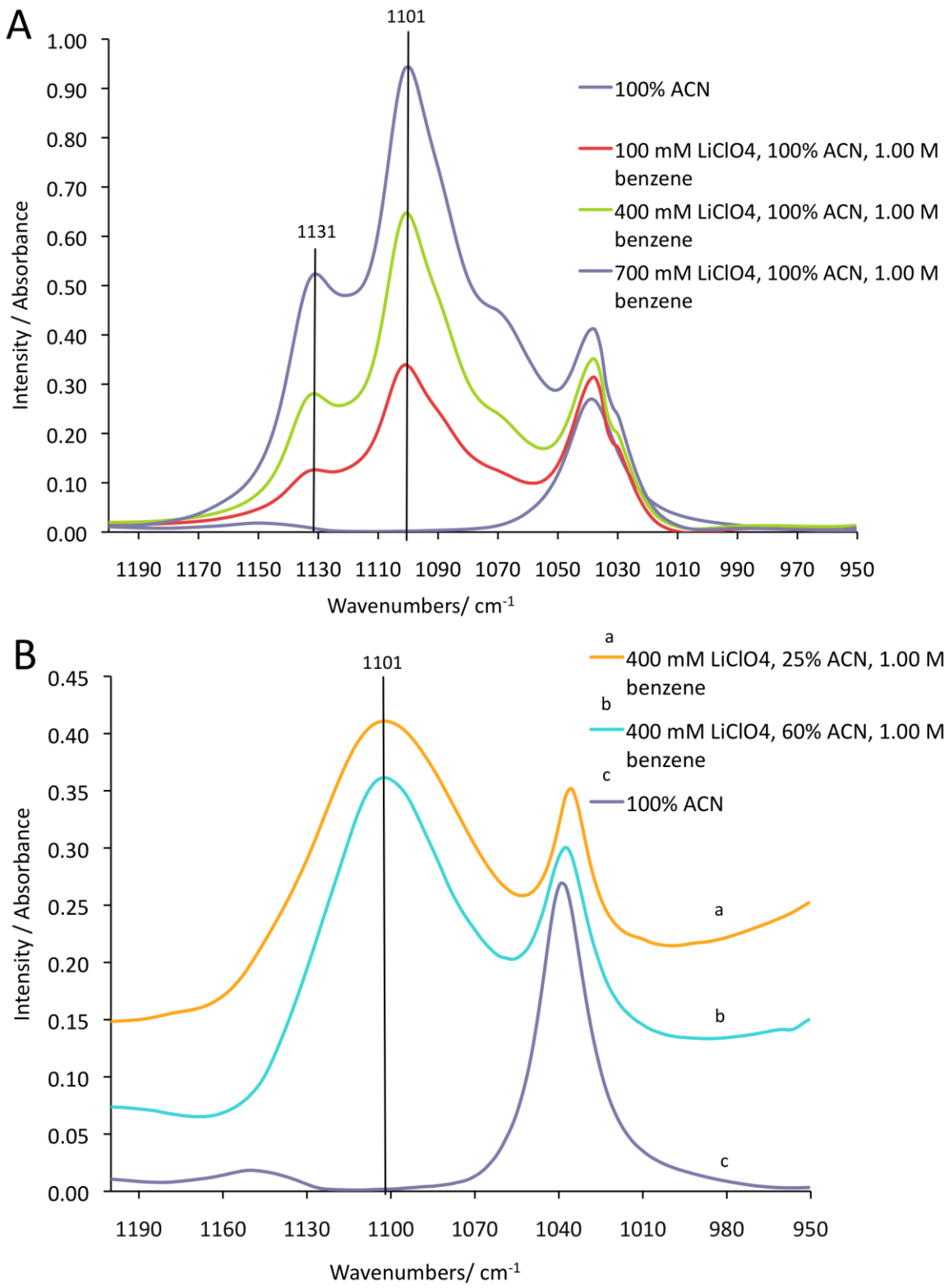

Figure 3-5. ATR-FTIR spectra of the CH_3 rock region (1250-950 cm^{-1}) for ACN in solutions containing 100 mM, 400 mM, and 700 mM $LiClO_4$ with 1.0 M benzene in 100% ACN (A) and 60% or 25% ACN (B). The spectra in (B) have been offset for clarity.

CHAPTER 4

CONCLUSIONS

The main objective of this thesis was to investigate the role of the organic modifier, acetonitrile (ACN) as an additive to an aqueous mobile phase in electrochemically modulated liquid chromatography (EMLC) to gain a better insight of the electrosorption process and in turn the retention mechanism. Chapter 1 gave a general introduction to EMLC, porous graphitic carbon (PGC), and the retention/electrosorption mechanism. Chapter 2 presented the effects of ACN on retention of aromatic sulfonates in EMLC. The results showed that ACN strongly alters the retention of aromatic sulfonates in mobile phases consisting of 20% ACN and greater due to ACN molecules forming a thick layer on the surface of the PGC, creating a pseudo-stationary phase. Through analysis of the Gibbs adsorption equation the interactions at the PGC was deduced. It was found, in mobile phases containing 20% ACN or greater that the retention mechanism is dominated by the solutes interacting with the pseudo-stationary phase through dispersive interactions. The interactions in the mobile phase were further investigated by using attenuated total reflection FTIR spectroscopy (ATR-FTIRS) in Chapter 3. These results gave an understanding of interactions occurring in the bulk solution prior to entering the electrical double layer in EMLC. It was found that a neutral, aromatic solute, benzene, formed hydrogen-bonds with water. The water molecules

formed a solvation shell around the benzene molecules; however, when the benzene concentration increased above 100 µM in solution a phase separation was observed due to repulsive forces between benzene and water. The supporting electrolyte had no observable interaction with benzene. However, ion association occurred between the supporting electrolyte ions and ACN depending on the presence of water.

Finally, these results serve as a basis for interpreting the electrosorption process. This work has implications to electrosorption phenomena outside of EMLC, e.g., the use of carbon electrodes in energy production and also as storage in fuels and batteries. Furthermore, the advancement in knowledge of the organic modifier in EMLC serves as a tool for chromatographers investigating problems in separations.